Tectonophysics 658 (2015) 74–90

Contents lists available at ScienceDirect

Tectonophysics

journal homepage: www.elsevier.com/locate/tecto

Liquefaction features at an archaeological site: Investigations of past earthquake events at the Early Christian Basilica, Ancient Lechaion Harbour, Corinth, Greece

Despina Minos-Minopoulos [a,b,*], Kosmas Pavlopoulos [a,c], George Apostolopoulos [d], Efthymis Lekkas [e], Dale Dominey-Howes [f]

[a] Harokopio University, Department of Geography, 70 El. Venizelou Str., Kallithea, 176 71, Athens, Greece
[b] Ephorate of Paleoanthropology & Speleology, Ministry of Culture, Education and Religious Affairs, Arditou 34B, 116 36, Athens, Greece
[c] Paris Sorbonne University Abu Dhabi, P.O. 38044 Abu Dhabi, UAE
[d] National Technical University of Athens, School of Mining and Metallurgical Engineering, Applied Geophysics Laboratory, 9 Iroon Polytechniou Str., Zografou, 157 80, Athens, Greece
[e] National and Kapodistrian University of Athens, Faculty of Geology and Geoenvironment, Department of Dynamic, Tectonic and Applied Geology, Panepistimioupolis Zografou, 157 84, Athens, Greece
[f] The University of Sydney, Asia-Pacific Natural Hazards Research Group, School of Geosciences, Sydney NSW 2050, Australia

ARTICLE INFO

Article history:
Received 4 September 2014
Received in revised form 9 April 2015
Accepted 23 July 2015
Available online 1 August 2015

Keywords:
Earthquake-induced ground liquefaction
Lateral spreading
Geophysical reconnaissance survey
Grain size distribution
Earthquake environmental effects

ABSTRACT

A synthesis of investigations carried out at the archaeological site of the Early Christian Basilica, located in the ancient harbour of Lechaion, Corinth, Greece in order to study the origin and triggering mechanism of deformation structures observed on the temple floor, is presented. These surface structures are indicative of earthquake induced ground liquefaction and their relationship with the subsurface soil stratigraphy and structure is examined. Investigations of stratigraphic data from archaeological excavations conducted from 1956 to 1965 provide indications of artificial fill deposits overlying a sandy-gravelly substratum. Geophysical survey of EM, GPR and ERT provided further information regarding the substratum properties/stratigraphy of the site indicating subsurface fissures and lateral spreading trends that are in agreement with the surface deformation structures. Lithostratigraphic data obtained from four vibracores drilled in the southern aisle of the temple, suggest estuarine deposits of coarse sand to fine gravel with grain size properties indicative of layers with high liquefaction potential. The results of the study, suggest at least three seismic events that induced ground liquefaction at the site. The first event pre-dates the construction of the Basilica, when Lechaion harbour was in operation. The second event post-dates the construction of the Basilica potentially corresponding to the regionally damaging A.D. 524 earthquake, followed by the third event, that commensurate with the A.D. 551 earthquake and the destruction of the temple.

1. Introduction and aims

The archaeological site of the ancient harbour of Lechaion is located on the southeastern coast of the Corinthian Gulf, 3 km to the west of the modern city of Corinth (Fig. 1a). Along with the Kenchreai harbour, it represents one of the harbours of the ancient city of Corinth. According to archaeological data, its construction dates to the 6th–7th century BC during the reign of Periander (Rothaus, 1995), and it remained operational throughout the Roman period (Pallas, 1959, 1965; Rothaus, 1995; Stiros et al., 1996). The harbour is located in a marsh, characterised by an outer harbour edged by moles and an inner artificially excavated harbour (cothon), connected to the Corinthian Gulf by a stone-lined channel (Fig. 1b). Continuous dredging activity is indicated by mounds of sand and pebbles located on the sand bar bounded at locations by retaining walls, separating the inner harbour basin from the outer harbour moles (Morhange et al., 2012; Pallas, 1960; Rothaus, 1995). During the late 5th to early 6th century A.D., an Early Christian Basilica was constructed on the western part of the sand bar separating the inner harbour basin from the coastline. The Basilica is thought to have only been in use for a short period of time since archaeological records suggest that it was destroyed by seismic activity in the mid 6th century A.D., (Pallas, 1956, 1959, 1960, 1965; Rothaus, 1995). This destruction is commensurate with extensive damage sustained in the region of ancient Corinth (Pallas, 1956; Rothaus, 1995; Scranton, 1957), and is thought to have been associated with the earthquake of A.D. 551 (Pallas, 1956, 1959, 1960, 1965).

* Corresponding author at: Harokopio University, Department of Geography, 70 El. Venizelou Str., Kallithea, 176 71, Athens, Greece.
E-mail addresses: dminou@hua.gr (D. Minos-Minopoulos), kpavlop@hua.gr, Kosmas.Pavlopoulos@psuad.ac.ae (K. Pavlopoulos), gapo@metal.ntua.gr (G. Apostolopoulos), elekkas@geol.uoa.gr (E. Lekkas), dale.dominey-howes@sydney.edu.au (D. Dominey-Howes).

http://dx.doi.org/10.1016/j.tecto.2015.07.010
0040-1951/

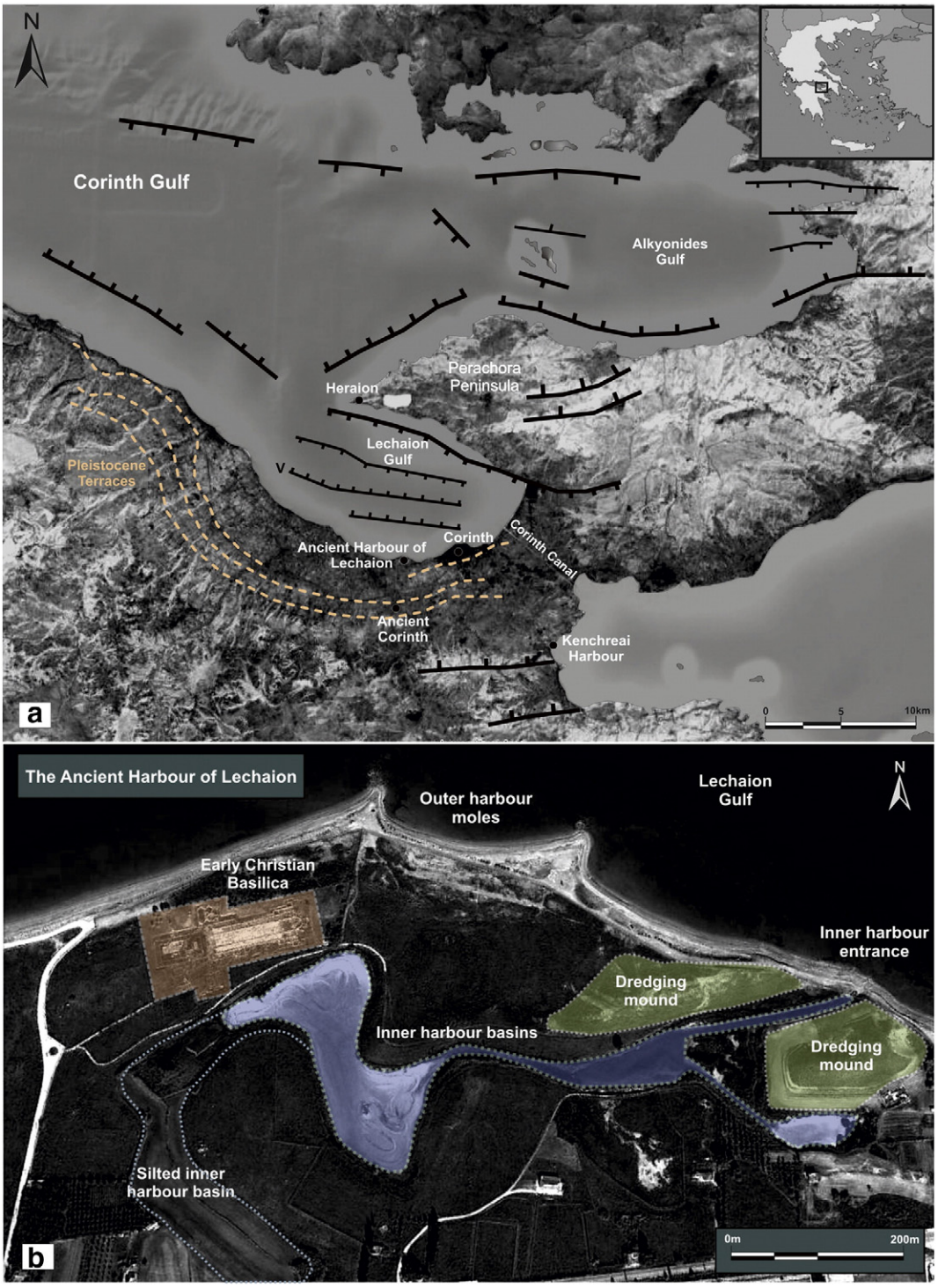

Fig. 1. (a) Map of the Corinth region, with location of study area, active faults after Sakellariou et al. (2007) and Charalampakis et al. (2014) and Pleistocene terraces after Armijo et al. (1996); V: Vrahati fault. (b) the Ancient Harbour of Lechaion and location of the Early Christian Basilica.

Recent restoration works carried out on the Early Christian Basilica have revealed the decorated floor of the temple that preserves deformation structures indicative of earthquake induced ground liquefaction. The aims of this work are to present and discuss the results of new investigations of the site in an attempt to study the surface deformation structures, confirm their triggering mechanism and propose a model of site evolution. To achieve the aims we first describe the geological setting, describe our methods and then present and analyse the results.

1.1. Geodynamic setting

The Corinth Gulf is an active continental rift system in a subduction zone setting, trending WNW–ESE, with extensional tectonics expressed through intense seismicity and marginal uplift. The east end of the rift is divided into two asymmetric sub-basins, the Alkyonides Gulf to the NE and the Lechaion Gulf to the SE separated by the fault bounded Perachora peninsula (Fig. 1a). The Lechaion Gulf, an asymmetric basin dipping to the north, represents an inactive relict of early rifting

(Leeder et al., 2005; Sakellariou et al., 2004; Turner et al., 2010). Spatial uplift rates of raised shorelines suggest fault slip related uplift for the Perachora peninsula of the order of 0.31 ± 0.04 mm/year since Marine Isotope Stage MIS 7 (Leeder et al., 2005, Turner et al., 2010). The southern margin (i.e. the northern Peloponnesian coast) is considered to be exhumed independent of fault slip and uplift of Pleistocene marine terraces is attributed to non-spatially uniform isostatic footwall uplift with rates ranging from 0.19 ± 0.05 mm/year to 0.31 ± 0.05 mm/year (Armijo et al., 1996; Leeder et al., 2003; Turner et al., 2010). Recent off-shore seismic studies carried out by Charalampakis et al. (2014) suggest that the Lechaion Gulf has a similar tectono-sedimentary evolution to the Alkyonides Gulf and that the Pleistocene uplift recorded along the southern coast is related to the activity of the Vrahati fault.

The geomorphology of the Corinth region is characterised by modest topography attributed to a flight of terraces presenting staircase morphology towards the Lechaion Gulf. These terraces are composed of Middle to Late Pleistocene marine sequences that lie unconformably on thick Plio-Pleistocene deposits of brackish to lacustrine marls, marly limestones, conglomerates and sands known as the Corinth Marls (Armijo et al., 1996; Keraudren and Sorel, 1987). The marine terraces represent glacio-eustatic transgression events during the Middle to Late Pleistocene that due to a complex combination of regional uniform isostatic with localised tectonic uplift are located at elevations that reach 400 m (Armijo et al., 1996; Keraudren and Sorel, 1987; Leeder et al., 2003; Turner et al., 2010).

Holocene coastal uplift is expressed via a series of raised shorelines in the Perachora peninsula suggesting multiple uplift events (Leeder et al., 2003; Pirazzoli et al., 1994; Turner et al., 2010) with the latest event of the order of 1.1 m dated to A.D. 190–440 as recorded in the vicinity of the archaeological site of Heraion (Pirazzoli et al., 1994). Late Holocene coastal uplift along the south coast of the gulf is suggested by exposed beachrock deposits along the coastline that at the western exit of the Corinth canal lie on top of ancient constructions (Mariolakos and Stiros, 1987) and by studies of Lechaion harbour.

Lechaion harbour is located in an estuary characterised by Holocene coastal and fluvial dynamics, with deposits varying from clays and silty sands to clean sands, gravels and conglomerates that at locations have been reworked by human activities (Morhange et al., 2012; Rothaus, 1995). Geomorphological and biological studies suggest active tectonics during antiquity through an episodic uplift of the order of ~1.1 m, that according to radiometric dating of marine organisms (Lithophaga) bored into raised walls of the harbour, is dated to circa 340 B.C. (Stiros et al., 1996). Supplementary radiometric data for this event comes from Morhange et al. (2012) suggesting uplift of the order of ~1.2 m around 375 ± 120 cal. B.C. This uplift event may have been followed by submergence of the outer harbour moles (Flemming, 1978; Turner et al., 2010; Vita-Finzi and King, 1985). Koster et al. (2011) using drill core sampling and GPR/ERT surveys identified what they proposed were tsunami deposits and abrasion scours in the western part of the harbour at a depth of 2 m. Additionally, Hadler et al. (2011, 2013) used geomorphological, sedimentological, geoarchaeological and geophysical data to identify at least three tsunamigenic events at Lechaion harbour and surrounding areas. According to radiocarbon dating, the first two events occurred about 760 cal B.C. and 50 cal A.D. respectively, while the youngest and most destructive event was dated to the 6th century A.D. This last tsunami was likely triggered by the A.D. 521 or 551 earthquake series and was related to the destruction of the Early Christian Basilica (Hadler et al., 2011, 2013). Mourtzas et al. (2014) suggest that sea level during the Roman period was 0.90 m lower than at present. After the Roman reconstruction of the ancient harbour installations in A.D. 358, two events of co-seismic submergence caused a rise of relative mean sea level by 1.60 m during the first event (A.D. 362–375) and by 0.40 m during the second (A.D. 522–580). These events were followed by either a strong uplift event or a sequence of smaller co-seismic uplift events that caused a relative sea level drop of the order of 1.10 m.

2. Methods

Liquefaction is the transformation of cohesionless, saturated, loosely packed sediments from a solid to a liquid state as a result of increased pore pressure and reduced shear stress, leading to ground failures due to hydraulic fracturing (Obermeier, 2009; Obermeier and Pond, 1999; Rodríguez-Pascua et al., 2015). During earthquake shaking, liquefaction occurs in sediments such as silt, sand and gravel, originating at a depth ranging from a few meters to about 10 m below the ground surface (Obermeier, 1996). Lateral spread, is the most common type of liquefaction ground failure in gently inclined grounds (Fig. 2) (Youd, 1984a; Andrus, 1986; Audemard M., 2002; Obermeier et al., 2005). The failure is expressed through vertical offsets and horizontal separations of blocks of surface soil along nearly vertical fissures that develop along a shear zone within the liquefied layer. Horizontal separation ranges from a few centimeters to several meters and develops on gentle slopes that range from 0.3% to 5% (Youd, 1984a, Bartlett and Youd, 1992; Obermeier et al., 2005). On slopes that exceed 3° or approximately 5% gradient, liquefied sediments can trigger landslides known as flow failures (Youd, 1984a; Obermeier, 2009).

Common surface failures include fractures and formation of localised depressions due to densification and settlement of liquefied sediment that can reach 0.25–0.5 m where thick sands liquefy severely (Obermeier, 1996). Circular depressions form along the length of fissures induced by seismic shaking in an impermeable cap (Obermeier, 1996). Such depressions according to Takahama et al. (2000), represent the final "draw-in" process in liquefaction that occurs just after an earthquake.

Another important characteristic of the ground liquefaction is recurrence. Liquefaction has the tendency not only to recur even at widely timed earthquakes, but also to use the same dikes for venting (Obermeier, 1996; Obermeier, 2009; Youd, 1984b). Investigations of liquefaction features and recurrence intervals have contributed to both palaeoseismological and seismic hazard assessment studies through earthquake magnitude–epicentre empirical relationships and their associations to the causative fault (Galli, 2000; Papathanassiou et al., 2005; Pavlides and Caputo, 2004; Rodríguez-Pascua et al., 2010; Audemard M. and Michetti, 2011).

Liquefaction features and their morphology have been identified and studied in archaeological sites as traces of palaeoearthquakes by combining archaeological records with stratigraphical and geophysical methods (Kanaori et al., 1993, Takahama et al., 2000, Sangawa, 2009; Karakhanyan et al., 2010; Tuttle et al., 2011). The application of these methods is considered valuable since it enables the relative dating of earthquake events through the association of liquefaction events with cultural layers (Barnes, 2010).

The methods employed in this study involve the combination of field observations and established geophysical surveys for earthquake-induced liquefaction features, with lithostratigraphic data from drill-

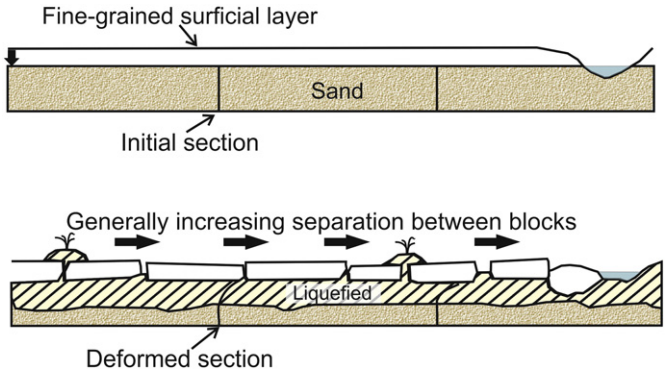

Fig. 2. Lateral spreading as a result of earthquake shaking on gently inclined ground near break in slope. Vertical arrow marks the water table level and sand venting through various types of fissures is indicated (modified after Youd, 1984a).

cores and existing archaeological records. The substratum investigation of the ground deformation structures observed on the decorated floor of the Basilica allows the study of the liquefaction features in relation to their surface expression providing relative indications for candidate earthquake event(s).

Field investigation included the mapping and cataloguing of distinct ground deformation structures where the floor was preserved in a good condition. The structures were positioned with differential GPS and were plotted into a rose diagram using the Stereonet software v. 9 (Allmendinger et al., 2012) in order to study their geometry, distribution and identify potential trends. The geophysical survey involved a combination of EM, GPR and ERT methods as a reconnaissance survey providing a fast, non-invasive method that allowed a thorough investigation of the study area with respect to the monument. The use of geophysical techniques for the detection and study of ground liquefaction structures has been used successfully (Abu Zeid et al., 2012; Al-Shukri et al., 2006; Liu and Li, 2001; Maurya et al., 2006; Tuttle et al., 2011; Wolf et al., 2006). The EM and GPR surveys along 10 ENE–WSW trending lines in the Basilica aimed to study the substratum properties such as grain size, permeability, saline water intrusions and compaction. The ERT survey included two profiles at right angles to each other in the Basilica on a NNW–SSE and NNE–SSW trend (Fig. 3) and detailed profiles of the upper 5 m were produced allowing a thorough study of the substratum deformation structures and their properties.

For the investigation of the lithostratigraphy, examination and synthesis of existing stratigraphic data described by Pallas during excavations carried out from 1956 to 1965 were performed, in order to reconstruct the archaeological stratigraphic succession, chronology and architectural evolution of the site and monument. The lithostratigraphy was further examined by four drill cores of short depth (Fig. 3 for locations) drilled along the southern aisle with a portable vibracore using 1 m and 2 m steel drill-pipes. The cores were located in the central part of the southern aisle where distinct depressions were recorded. Cores 2 and 4 were positioned in circular depression structures in the floor while cores 1 and 3 were positioned in surrounding locations where the floor was considered as relatively undisturbed. The aim of this method was to identify potential lithostratigraphic variances, properties and characteristics among disturbed (depressions) and relatively undisturbed substratum that could relate to ground liquefaction. Sampling was conducted according to colour and grain size variations observed and a total of 40 sediment samples were analysed. The core profiles were determined through laboratory sieve analysis tests. The samples were dried and sieved through the standard sieving column with meshes ranging in diameter from 40 mm to 0.063 mm. All analyses were conducted in the Department of Geography, at the Harokopio University. The grain size distributions, median diameter, sorting, skewness and kurtosis were calculated as logarithmic graphical measures using Folk and Ward (1957) formulae through the Gradistat program (Blott and Pye, 2001).

3. Results

3.1. Field investigations

Observations and measurements occurred in parts of the temple where the decorated floor was preserved in a good condition allowing clear observation of the deformation structures. The dimensions, geometry and distribution of the ground deformations recorded correlate well with the surface expression of liquefied granular deposits (Obermeier, 2009; Tokimatsu and Seed, 1987).

The well-preserved southern aisle contains numerous circular and linear depressions concentrated mainly at the northern side of the aisle striking ENE–WSW (Fig. 4a) oriented nearly parallel to the Basilica walls. Dimensions vary from 0.45 × 0.33 m and 0.12 m depth to 1.80 × 1.33 m and 0.4 m depth for the circular depressions (Fig. 4b) while the linear depressions (Fig. 4d) have a variable depth ranging from 0.05 to 0.12 m and lengths that range from approximately 0.5 to 1 m. Some of these linear structures are in contact with the circular depressions (Fig. 4c). In the central aisle, where the floor is not preserved in a good condition, scattered linear and circular depressions were recorded, along with linear and circular buckling structures (Fig. 5). Due to the poor preservation of the floor it was not easy to identify a trend in the distribution of the circular depressions other than for some clustering recorded in the central part and near the limit with the southern aisle. However, a primary trend was identified with the majority of the linear features striking NNW–SSE, at right angles to the strikes recorded in the southern aisle, followed by a secondary less extensive ENE–WSW trend running near parallel to the trend of the Basilica walls.

Where the floor was not preserved it was difficult to identify and measure deformation structures. Some large-scale circular depressions were identified and recorded but potential linear depressions that were not preserved in a good condition were not included in our records. The northern aisle was covered with gravel and soil during our research and so it was not possible to identify surface ground deformation structures. However, the aisle was uncovered after our work and although only limited deformation structures were observed that were restricted to circular depressions, this provided useful additional information presented and discussed in Section 4.

Plotting the linear depressions and buckling structures recorded on the central and southern aisle of the temple into a rose diagram (Fig. 6), indicate a primary trend of ENE–WSW strike and a secondary trend of NNW–SSE strike. The linear features with ENE–WSE strike, are oriented at a near parallel trend in relation to the coastline and inner harbour basin shore, while the secondary NNW–SSE strike is

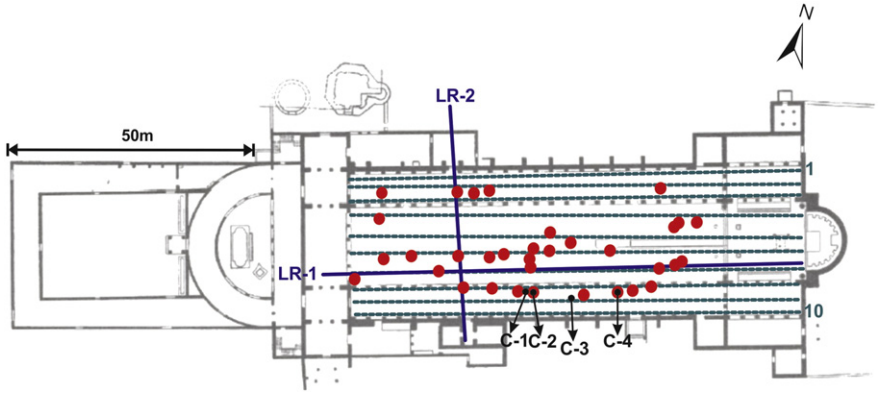

Fig. 3. Location of the 10 EM and GPR profiles (dashed green lines), the two ERT profiles (purple lines), the location of distinct deformation structures (red dots) and drill cores (black dots) in the Early Christian Basilica.

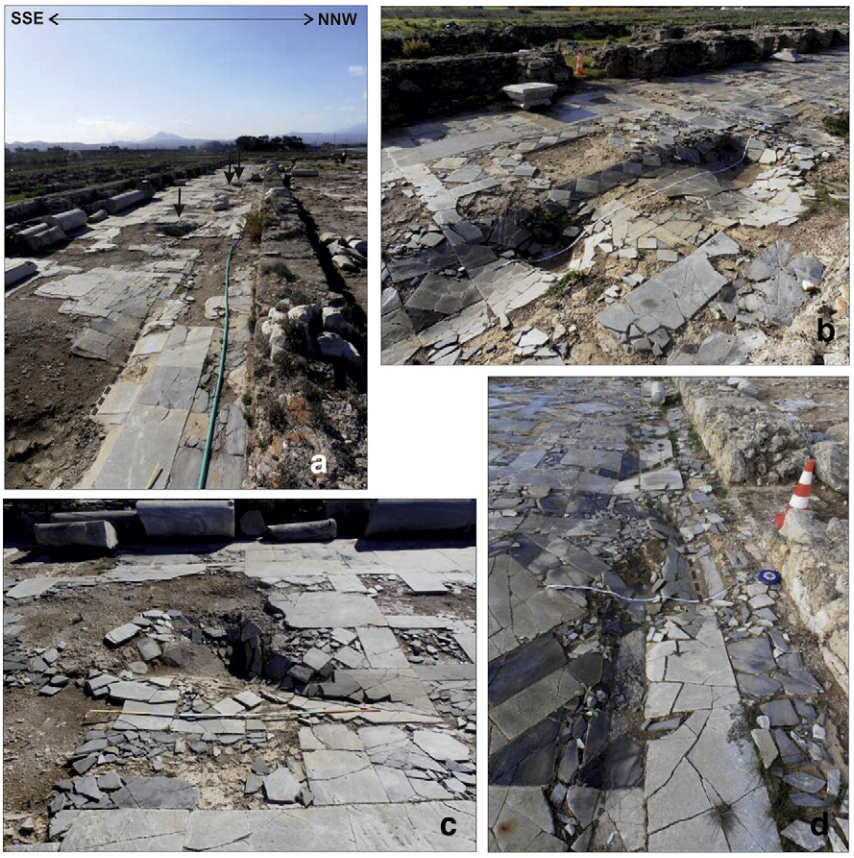

Fig. 4. Deformation structures recorded on the southern aisle of the Early Christian Basilica, (a) circular depressions (black arrows) and linear depression (dashed line) in a ENE–WSW trend, (b) two characteristic circular depressions, (c) linear depression in contact with a circular depression, (d) linear depressions indicated by dashed line.

oriented at a parallel trend in relation to topographic depressions located to the SW and NE of the Basilica and at right angles to the primary strike, indicating predominant topographic control of ground deformation (Obermeier, 2009).

3.2. Archaeological stratigraphic succession

The subsurface lithostratigraphy of the Basilica presented in Fig. 7, represents a synthesis of the stratigraphic data described by Pallas during original site excavations from 1956 to 1965. Trial trenching (Pallas, 1959, 1960, 1965) was carried out at two sites in the Basilica floor (trenches 1 and 2) and surrounding locations (3, 4, 5 and 6).

The outer foundations of the Basilica as observed in trial baulk (trench 3) and trench 4 reach a depth of 1.20 m, while the inner foundations according to trench 1 reach down to 1.70 m.

The Basilica was founded on a sandy substratum located at approximately 1 m below the floor of the temple (trenches 1, 3 and 4) and according to two Corinthian coins found on the excavation baulk (trench 3), it dates to the 3rd century B.C. A layer of angular calcareous sandstone boulders mixed with sand was recorded in trenches 5 and 6 located to the SW of the Basilica extending from 1.45 m to 2.40 m below the ground surface. This layer represents an artificial deposit possibly related to early harbour installations (Pallas, 1959). Although the continuation of this layer under the Basilica is unknown, its existence is indicative of potential artificial fill deposits extending to a depth of 3 m (Pallas, 1960). Therefore, since the surroundings of the Early Christian Basilica represent ancient harbour installations potentially dating back to the 6th–7th century B.C. it is not clear whether and to what extent, the sandy substratum represents natural or artificial deposits.

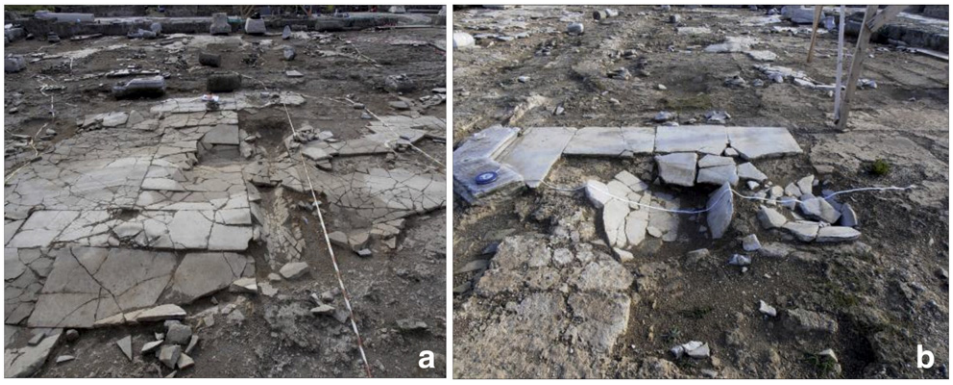

Fig. 5. Ground deformation including buckling structures (a) and depressions (a and b) in the central aisle of the Early Christian Basilica.

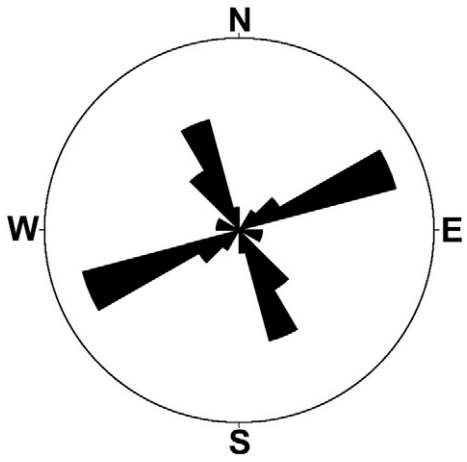

Fig. 6. Rose diagram of linear fractures trends as recorded on the Early Christian Basilica decorated floor. The ENE–WSW set is dominant followed by the NNW–SSE set.

The preparation ground for the construction of the Basilica, overlying the sandy substratum is composed of silty sand layers locally containing fragments of calcareous sandstone and rubble of mortar, ceramic tiles and marble (trenches 1 and 2). The horizon has a thickness of ~0.5 m as recorded in trench 1 and according to an Assarian coin of Theodosius B′ (A.D. 408–450), it is dated to the mid 5th century A.D. The coin correlates well with the two coins found in the trial baulk in artificial fill deposits suggesting that the foundation of the Basilica occurred in the mid 5th century A.D. (Pallas, 1965).

The stratigraphy that overlies the preparation ground horizon represents the artificial fill used during the works of levelling the floor of the Basilica (Pallas, 1960, 1965). This levelling horizon is composed of layers of sand bearing pebbles and clay as observed in trial trench 1 while in trench 2; it is composed of "tight pressed soil" (Fig. 7). In trench 1, the upper parts include lithic fragments, while trench 2 partly contains rubble of ceramic tiles and mortar.

According to a coin of Ioustin A′ (A.D. 518–527) found in trench 2, the artificial fill is dated to the early decades of the 6th century A.D. (Pallas, 1965). It is interesting to note that this coin, located at approximately 0.90 m depth near the foundation ground horizon, comes in contrast with the dating associated with coins from similar depth horizons that date to approximately 70 years earlier. It is noteworthy, that the stratigraphy in trench 2, towards the south, is interrupted by a vertical discontinuity composed of ceramic tiles, mortar and marble rubble containing in its upper parts coarse-grained sand with pebbles. The coin is located above the foundation ground horizon, at 1.10 m depth in "tight pressed soil" deposits. The existence of this coin at such a depth was interpreted by the archaeologist as a *terminus post quem* for the levelling of the ground and the construction of the decorated floor (Pallas, 1965). Archaeological findings before the excavation of trench 2 indicated tiling of the floor towards the end of the 5th century A.D. The coin of Ioustin A′ led to the transposition of this date to approximately three decades later (Pallas, 1965). It is suggested that this stratigraphic discontinuity directly relates to the chronological discontinuity, as will be discussed in Section 4.

A summary of the subsurface stratigraphy of the Basilica from top to bottom includes an artificial fill composed mainly of sand and pebbles with occasional intercalations of clay, lithic and ceramic tiles fragments and mortar. This fill extends to a depth of a least 1 m below the Basilica

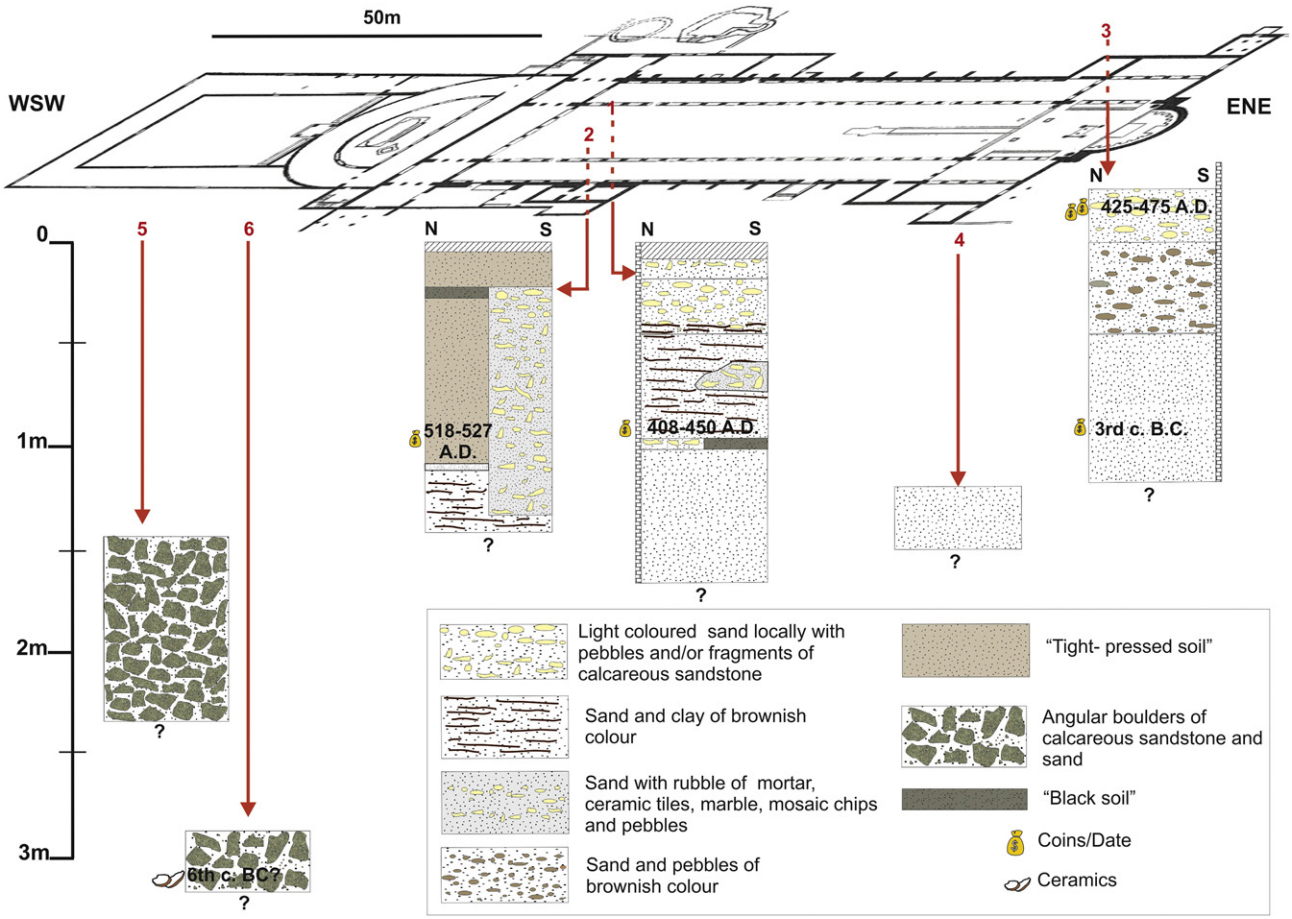

Fig. 7. Lithostratigraphic synthesis according to archaeological trial trench observations within the Basilica (1, 2) and surrounding locations (3, 4, 5 and 6), after Pallas (1956, 1959, 1960, 1965).

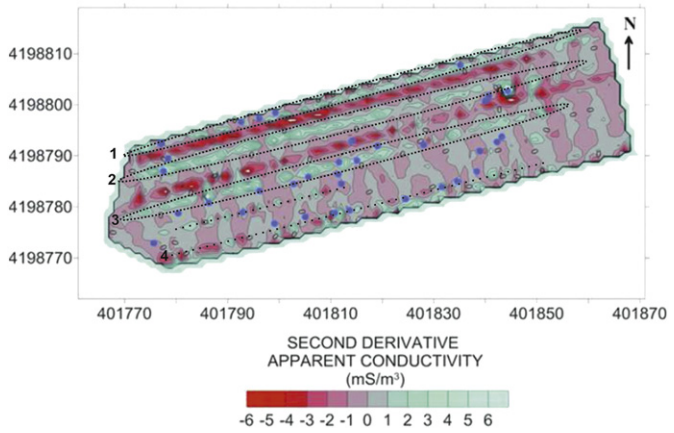

Fig. 8. The EM map of the second derivative of apparent conductivity at 3 m depth. Blue dots indicate recorded surface deformation structures. The three principal high conductivity zones are shown with dashed circles while the potential fourth zone is indicated by the dashed line.

floor and its lower layer is considered as the preparation ground for the construction of the Basilica. The foundations of the temple are located at depths of 1.45 m and 1.70 m in sand deposits that date to the 3rd century B.C. As suggested by the existence of a layer of boulders at 3 m depth located to the SW of the Basilica, the artificial nature of the subsurface stratigraphy possibly extends to a depth of 3 m.

3.3. Geophysical survey

The geophysical survey provides information regarding the sedimentary properties and structural characteristis of the substratum. The EM map for effective depth range of 1.5 m suggests more conductive fine-grained deposits in the western part of the temple in relation to the eastern part that appears less permeable and coarse-grained (Apostolopoulos et al., 2013). The GPR survey allowed the identification of the sea water level at an approximate depth of 3 m and the existence of numerous interfaces of coarse deposits at the eastern part of the temple that are in agreement with the EM measurements. The ERT profiles were indicative of a coarse resistive upper stratum that lies on fine-grained conductive sandy deposits.

Substratum structures related to earthquake induced ground liquefaction features were identified with all three geophysical methods. The ERT profiles are indicative of a relatively coarse grained resistive upper layer of 4 m thickness interrupted by vertical, relatively less resistive fine-grained conductive sand zones. These zones develop in both profiles within the Basilica and are in good correlation with both the GPR and EM features and with surface deformation structures, suggesting liquefaction sediment source at 4–5 m depth and lateral spread geometry that develops in a general primary ENE–WSW trend (LR-2) and a NNW–SSE secondary trend (LR-1).

More specifically, with the EM method, three linear relatively higher conductivity zones with an ENE–WSW trend were identified on the second derivative conductivity map of 3 m effective depth range (Fig. 8), running parallel to two linear relatively lower conductivity zones. The lower conductivity zones possibly represent deposits related to harbour constructions that pre-date the Basilica construction, while the higher conductivity zones being in good agreement with surface deformation structures are indicative of lateral spreading fissure zones. These higher conductivity zones appear more continuous in the northern aisle (zones 1 and 2), while in the central part of the central aisle (zone 3) appear less continuous. In the southern aisle the existence of a potential fourth higher conductivity zone is indicated (zone 4), mainly by the linear distribution of localised conductivity maxima in the EM contours that are in good correlation with the distribution of surface circular depressions and linear fractures.

The zones with the primary ENE–WSW trend were also identified in the ERT LR-2 profile section oriented at right angles to them, as indicated in the detailed profile of the upper 5 m (Fig. 9). The three linear conductive zones are represented in the LR-2 profile by near vertical fine grained, lower resistivity zones in the coarse resistive upper stratum. These discontinuities express the fragmentation of the upper stratum indicating maximum displacement up to 3 m at the northern part of the temple (zone 1), suggesting settlement and lateral extension towards the SSE. The zones 2, 3 and 4 are not as clear in the profile as they appear in the EM map but their existence is indicated by narrower, less resistive, near vertical zones that correlate with surface deformation structures. These narrower zones are indicative of a relatively

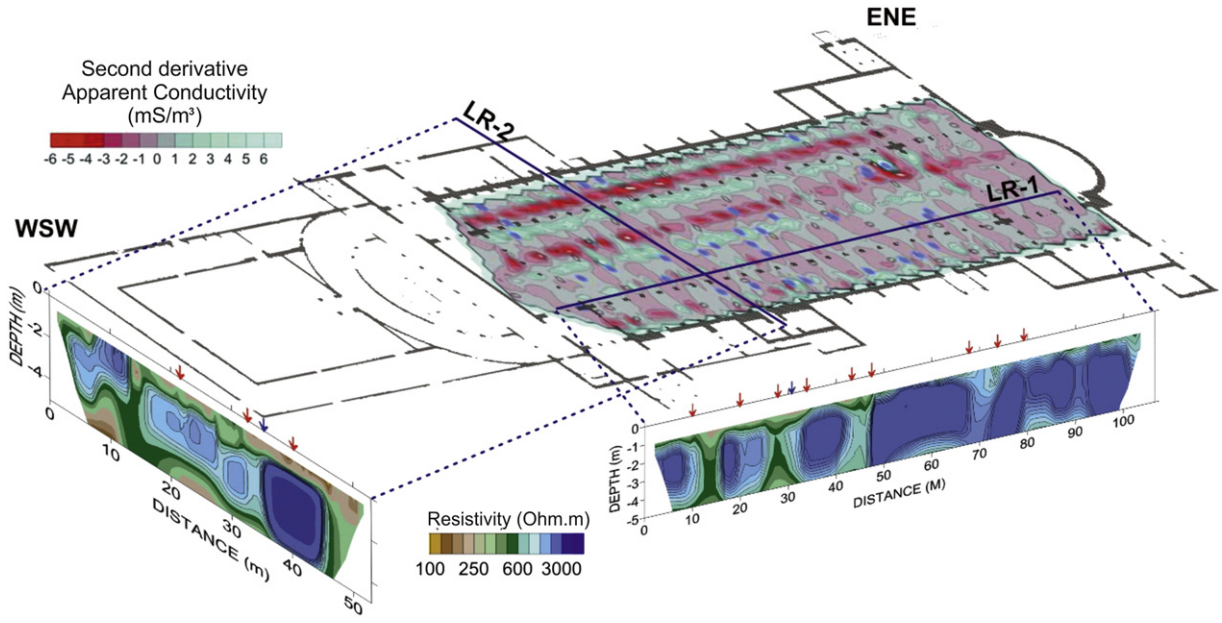

Fig. 9. The Early Christian Basilica plan with the EM second apparent conductivity map of 3 m effective depth range and projections of the two detailed ERT profiles (LR-1 and LR-2). Blue dots indicate the ground deformation structures recorded on the surface, indicated with red arrows on the ERT profiles. Blue arrows indicate the intersection of the two ERT profiles.

small-scale vertical downward displacement of a resistive upper stratum block, forming a small graben.

The physical characteristics and spatial arrangement of these zones and their correlation with the deformation structures recorded on the Basilica floor and the geomorphological setting, suggest that they represent lateral spreading fissure zones (Abu Zeid et al., 2012), originating as tension breaks in response to the lateral displacement. The lateral spread fissure zones that develop in a primary ENE–WSW trend, as interpreted by the LR-2 ERT profile and EM map of the second derivative of apparent conductivity, exhibit a trend near parallel to the coastline and the inner harbour shore suggesting a downslope horizontal displacement towards the SSE free face of the inner harbour shore, along a shear deformation zone located at approximately 4 to 5 m depth (Youd, 1984a).

Potential secondary substratum zones of relative moderate conductivity values with a NNW–SSE trend are also indicated in the second derivative of the apparent conductivity map of 3 m effective depth range that appear mostly in the central and southern aisle of the temple. These zones correlate well with the LR-1 ERT profile (Fig. 9) that indicates nearly vertical discontinuities up to 2–3 m wide in the WSW part of the profile and narrower less resistive discontinuities in the ENE part of the profile. Again, the surface deformation structures are in good agreement with these zones as indicated in the detailed section of the upper 5 m of LR-1 suggesting secondary near vertical fissure zones and liquefaction source sand horizon below 4 m depth. Their relationship with the primary fissure zones is not clear. They could either represent topographically controlled lateral horizontal displacement of the upper dense stratum towards the WSW, a trend supported by the downslope topography to the west of the Basilica (Youd, 1984a), or they could represent secondary structures triggered by the manifestation of the vertical displacements along the primary fissure zones (Coulter and Ralph, 1966).

Good correlation of surface deformation structures with vertical zones of low signal amplitude in the upper 3 m of the GPR profiles and near vertical lower resistivity zones in the coarse resistive upper stratum of the ERT profile (Fig. 10) suggests sand vent features and liquefaction sediment source below the water table level at 3 m depth (Fig. 10c).

As indicated by the geophysical survey, a failure zone is located at depths of 4–5 m. This failure zone is a relatively fine-grained sedimentary horizon lying under a dense coarse-grained stratum of approximately 4 m thickness. This horizon is located approximately 1–2 m below the water table and could be considered as the most susceptible horizon to liquefaction. The behaviour of this fine grained horizon as a shear zone is supported by the vertical fracturing of the overlying stratum through fissures that root in this horizon filled with sediment of similar properties, suggesting upward venting of liquefied sediment resulting to the lateral displacement of overlying strata through zones of lateral spread. The locations of the fissures and lateral spreading trends correlate well with surface deformation structures on the Basilica floor striking in primary ENE–WSW and secondary NNW–SSE directions, oriented near parallel to surrounding topographic declivities.

3.4. Coring

3.4.1. Lithostratigraphy

From the lithostratigraphic analysis of the samples from the four vibracores, three sedimentary units were identified, the artificial Unit A and the sedimentary Units B and C characterised with caution as “natural” since they could represent artificial fill deposits of the ancient harbour installations (Fig. 11). The stratigraphy of the four cores is summarised in Table 1. Note that the stratigraphy in cores 2 and 4 starts at 0.315 m and 0.34 m depth respectively since these cores were positioned in circular depressions.

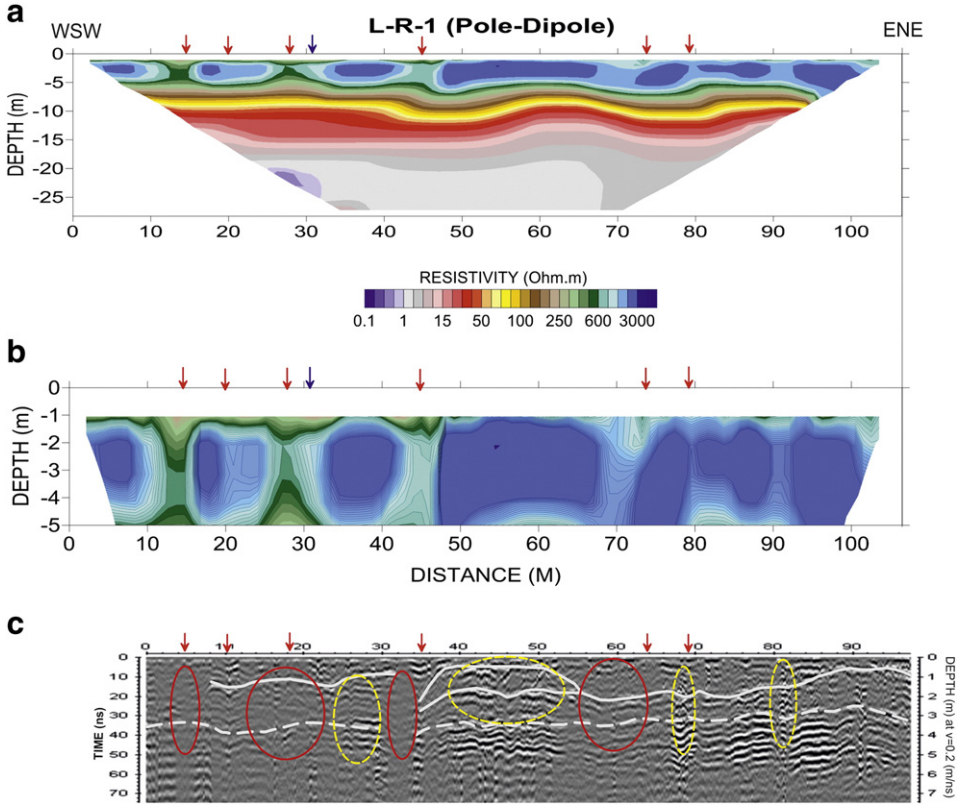

Fig. 10. The LR-1 ERT profile (a) with a detailed section of the upper 5 m (b) and the 7th GPR profile (c). Red arrows correspond to surface deformation structures that correlate with near vertical fissures. Yellow dashed line circles in the GPR indicate coarser grained deposits in relation to the red solid line circles that indicate finer grained deposits. White dashed line corresponds to water table level and continuous lines to potential distribution of artificial fill deposits.

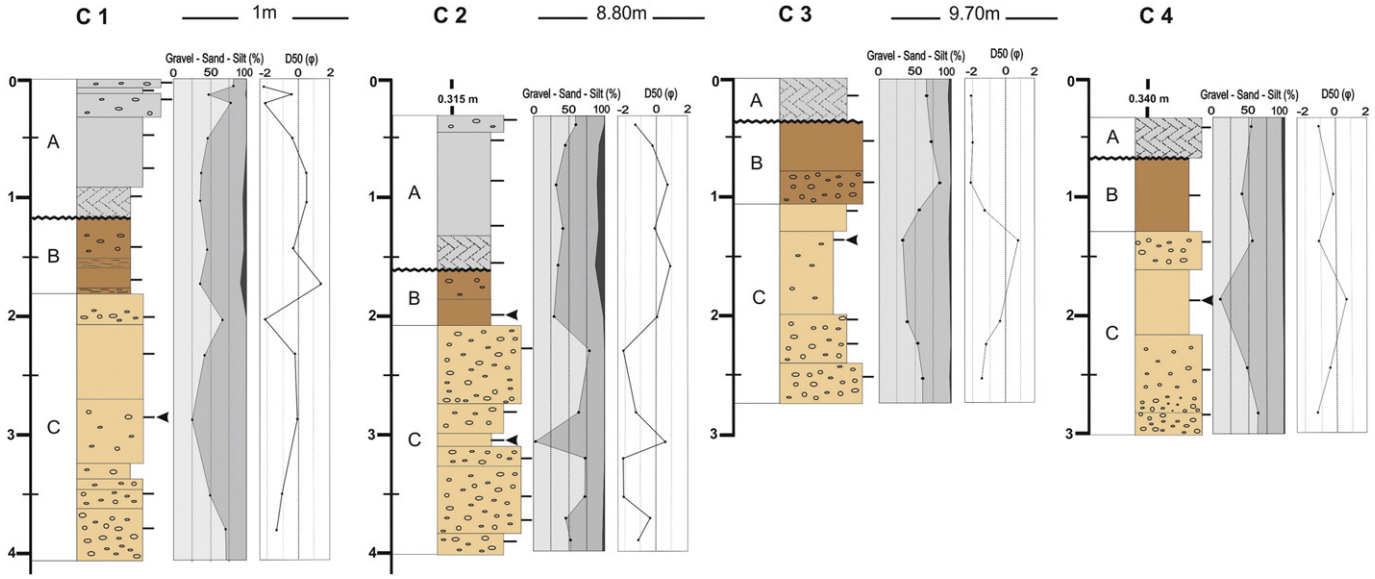

Fig. 11. Geological columns of the two sets of boreholes, with grain size content and mean D_{50} (φ). The horizontal distance between boreholes is indicated at the top of the figure. Bold wavy line indicates the unconformity that represents a "palaeosurface" between Unit A and Unit B. Black triangles indicate layers with high potential for liquefaction.

3.4.1.1. Unit A—artificial fill. The upper deposits of Unit A are composed of relatively packed coarse to very coarse sand layers with fine gravel and pebbles. They are recorded only in cores 1 and 2 with a thickness of 0.9 to 1 m, while they are absent in cores 3 and 4. These deposits correlate well with the artificial fill layers described in archaeological trenches 1, 2 and 3, that according to coins date to the late 5th c. A.D., with the exception of the deposits in trench 2 dated to the early 6th c. A.D.

3.4.1.1.1. Base layer—preparation ground for the construction of the Basilica. All four cores contain a packed layer of dark grey colour with a thickness of 0.22–0.37 m containing fragments of ceramic tiles and agglomerates. This layer appears as base layer to the artificial fill in cores 1 and 2 recorded at 1.18 m and 1.53 m depth respectively, while it appears as the surface layer in cores 3 and 4. Its composition has similar characteristics in all four cores; in cores 1 and 2 it is composed of very poorly sorted coarse sand, has a symmetrical skewness and is platykurtic, while in cores 3 and 4 it is composed of poorly sorted very coarse sand, that is very finely skewed and platykurtic. Median D_{50} ranges from 0.932 φ in core 2, to −2.068 φ in core 3. The presence of ceramic tiles fragments and agglomerates in this layer and its stratigraphic location under the artificial fill are strong indications suggesting a direct correlation with the archaeological layers related to the preparation ground for the construction of the Basilica (Fig. 7). This layer that according to the archaeological stratigraphy is dated to the mid 5th c. A.D., represents the boundary between upper Unit A and the underlying Unit B with their contact expressed through an unconformity (wavy line between Units A and B in Fig. 11). This unconformity represents a "palaeosurface" potentially relating to the use of the harbour during antiquity.

This layer allows the following observations:

1. The "palaeosurface" before the construction works of the Basilica according to the distribution of its stratigraphic depth (Fig. 11) was gently dipping towards the west.
2. In core 2, the layer is located approximately 0.35 m below the level of the layer in core 1. This difference correlates well with the surface circular depression depth of 0.31 m, suggesting that the liquefaction occurred below the "palaeosurface" resulting in vertical displacement and settlement of both the preparation ground layer and the overlying artificial fill deposits. A similar direct displacement is also indicated by the same layer in core 4. In this core the absence of the artificial fill suggests settlement of the order of 0.34 m directly attributed to the underlying stratum.

3.4.1.2. Unit B—upper "natural" sand. The upper "natural" sand underlies Unit A. Its maximum thickness of 0.7 m, is recorded in core 3. It is composed of poorly sorted fine skewed coarse sand layers bearing pebbles. However, in core 3 it appears coarser and in core 1 intercalations of silty sand were recorded. In cores 1 and 4 the sediment is platykurtic while in cores 2 and 3 is leptokurtic. Median D_{50} ranges from −2.105 φ recorded in core 3 to 1.517 φ in core 1. Unit B is considered as "natural" in relation to the overlying Unit A since it does not contain archaeological findings. However, no clear indications exist to allow discrimination of natural from artificial processes of deposition. The depth of the upper "natural" sand especially in cores 1 and 2 correlates well with the sand horizon of the Basilica foundation ground as described in the archaeological trenches 2 and 1 respectively

Table 1
The stratigraphic units with their depths for each core.

Stratigraphy		Depth			
Unit	Deposits	Core 1	Core 2	Core 3	Core 4
A	Artificial fill	0–0.90	0.315–1.32 m	–	–
	Basal layer	0.90–1.18 m	1.32–1.53 m	0–0.37 m	0.34–0.68 m
B	Upper "natural" sand	1.18–1.80 m	1.53–2.07 m	0.37–1.07 m	0.68–1.31 m
C	Lower "natural" sand	1.80 m–4.06 m	2.07 m–3.98 m	1.07 m–2.75 m	1.31 m–2.97 m

while cores 3 and 4 correlate well with the archaeological trial trench 4 and the trial baulk layer (trench 3) that is dated to the 3rd century B.C.

3.4.1.3. Unit C—lower "natural" sand. Unit C is also considered as relatively "natural" compared to the overlying Unit A for the same reasons as in Unit B. In cores 1 and 2, the unit develops below 1.80 m and 2.07 m depth while in cores 3 and 4 it is recorded below 1.07 m and 1.31 m respectively. It is composed of poorly sorted coarse sand to fine gravel layers with variable skewness and kurtosis. Median D_{50} ranges from −2.141 in core 2 to 0.745 in core 3. This layer does not correlate with any archaeological layer from the excavations in the Early Christian Basilica since the trial trench excavation depth was limited to the depth of the foundations of the temple. However, since Unit C is located under the unit dated to the 3rd. c. B.C. it can be suggested that Unit B represents chronologically the *terminus ante quem* for Unit C.

In general, the grain size distribution of the deposits ranges from poorly to very poorly sorted coarse, silty sand to very fine gravel bearing pebbles with maximum dimensions of 2–3 cm and median D_{50} ranging from −2.174 to 1.517 φ. The fines content is minimal in cores 3 and 4 ranging from 0.2% to 3.2% with maximum values observed near the surface, while in cores 1 and 2 the content of fines increases in the upper 2 m of the cores reaching maximum of 10%.

The skewness ranges from very fine to symmetrical with only one coarse skewed layer that is preserved in cores 1, 3 and 4 (Fig. 12). Kurtosis varies from very platykurtic to very leptokurtic. In addition the sediments appear in general as polymodal suggesting composite distribution and sediment mixing (Curray, 1960). It is not clear if this sediment mixing is natural or artificial since the continuous use of the site as a harbour suggests works and interventions that could include artificial fill deposits. Nonetheless, the stratigraphical properties suggest a mixing of high energy fluvial sediments reworked by shallow water marine processes representing estuarine depositional environment (Friedman, 1967), as indicated in Fig. 12.

3.4.2. Liquefaction source sand

Grain size distribution is considered as a useful tool for the identification of liquefaction sand and horizons through the cumulative frequency curves (Andrus, 1986; Inoue et al., 2006; Tsuchida and Hayashi, 1971). Modal and median diameter values (Inoue et al., 2006) have also been utilised for the identification of liquefied and jetted sand deposits although it is not considered as a method to be used in isolation.

From the analysis of the samples from each unit (Fig. 13), the cumulative frequency versus grain size diagrams suggests that all deposits are potentially liquefiable according to the liquefaction boundary curves suggested by Tsuchida and Hayashi (1971). Therefore, the core samples suggest potential liquefaction deposits but no direct indications for a potential liquefaction horizon.

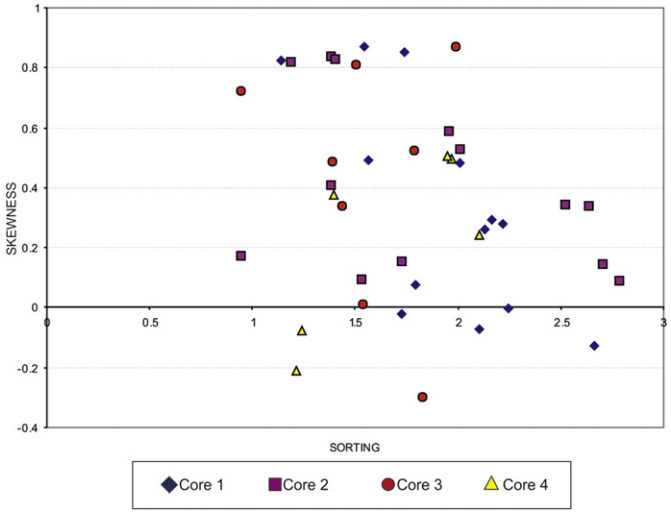

Fig. 12. Plot of skewness versus sorting for the samples from all four cores indicating estuarine depositional environment (Friedman, 1967).

However, at least one curve in each core can be considered as most liquefiable according to the liquefaction boundary curves. The primary observation is that these deposits are recorded in Unit C. In cores 2 and 4, in the deposits of Unit C, samples L2-9 and L4-4 respectively stand out in the cumulative frequency diagrams since they can be considered as most liquefiable (Fig. 14).

The samples are coarse-grained sand layers with D_{50} of 0.6 φ and primary mode of 0.75 φ. They are relatively less poorly sorted compared to the rest of the deposits and stand out in the sorting versus mean grain size graph (Fig. 15). The L2-9 is located at a depth of 2.99–3.12 m and is described as yellowish brown coarse sand with 97% sand, 2.7% gravel and 0.2% clay that is fine skewed, moderately sorted and leptokurtic. This sample represents a thin layer of 0.13 m thick of coarse sand with median D_{50} of 0.6 φ, that appears as a lamination in a thick layer of very fine gravel and very coarse sand that extends below 2 m depth. This coarse sand layer is located at the present water-table level at 3 m depth. Sample L4-4 is located at a depth of 1.80 to 1.90 m and has 89.6% sand, 10% gravel and 0.4% clay; it is poorly sorted yellowish brown coarse sand, symmetrically skewed and very leptokurtic. The sample was taken from a layer of very coarse sand of median D_{50} of 0.65 φ that has a thickness of 0.55 m and extends from 1.62 m to 2.17 m depth.

Layers with D_{50} values, primary modes and cumulative frequency curves close to these two samples have been identified in all four cores (Fig. 16). In core 1, sample L1-11 represents a layer 0.55 m thick of very poorly sorted very coarse sand with median D_{50} of 0 φ and primary mode of 0.75 φ located at 2.70 to 3.25 m depth. In core 2, sample L2-6 located in a layer of poorly sorted coarse sand at 1.87–2.09 m depth and 0.22 m thick also has a D_{50} of 0 φ and primary mode of 0.75 φ. Finally in core 3, sample L3-5 which is a poorly sorted coarse sand layer located at 1.30–2.01 m depth has a median D_{50} of 0.76 φ and primary mode of 0.75 φ (Fig. 11). Although these samples are coarser than L2-9 and L4-4 (Fig. 15), the primary mode is the same and their cumulative frequency curves present a similar curve sinuosity. With the exception of layer L2-6 that is located in Unit B, all the rest of the samples are located in Unit C. Although these layers could be considered as representing the liquefaction source sand, we are not in a position to suggest that these layers represent the liquefaction sand horizon since their stratigraphic distributions at different depths, their variable thickness and the characteristics of the underlying and overlying sediments suggest that they possibly represent fissure fill deposits (Obermeier, 2009) and that the liquefaction sand horizon is located deeper in the strata below 4 m depth. This potential liquefaction sand horizon depth is in agreement both with the geometry and the properties of the deposits as presented in the ERT profiles LR1 and LR2.

In addition, although samples L2-9 and L4-4 represent sand with the highest potential for liquefaction, their grain size distribution cannot be directly correlated with grain size distributions of the top layer samples in cores 2 and 4.

In general, liquefaction dike fillings can vary in grain size from silty fine sand to gravelly sand with fines up to 10% and are considered as structureless (Obermeier et al., 1993). In addition, the dike fillings in many instances contain clasts of sidewall material that were transported upwards. When coarse sand and gravel is present, there is generally a fining upward sequence that does not allow the direct correlation of liquefied horizons with sand boil ejecta (Cao et al., 2011; Obermeier et al., 1993).

In lack of sand boil ejecta that were probably removed during the archaeological excavations and during the recent restoration works at the site, an investigation of the top layer samples in cores 2 and 4 was carried out in order to examine their properties and their potential relation to the liquefied sand layers. It should be noted that a considerable

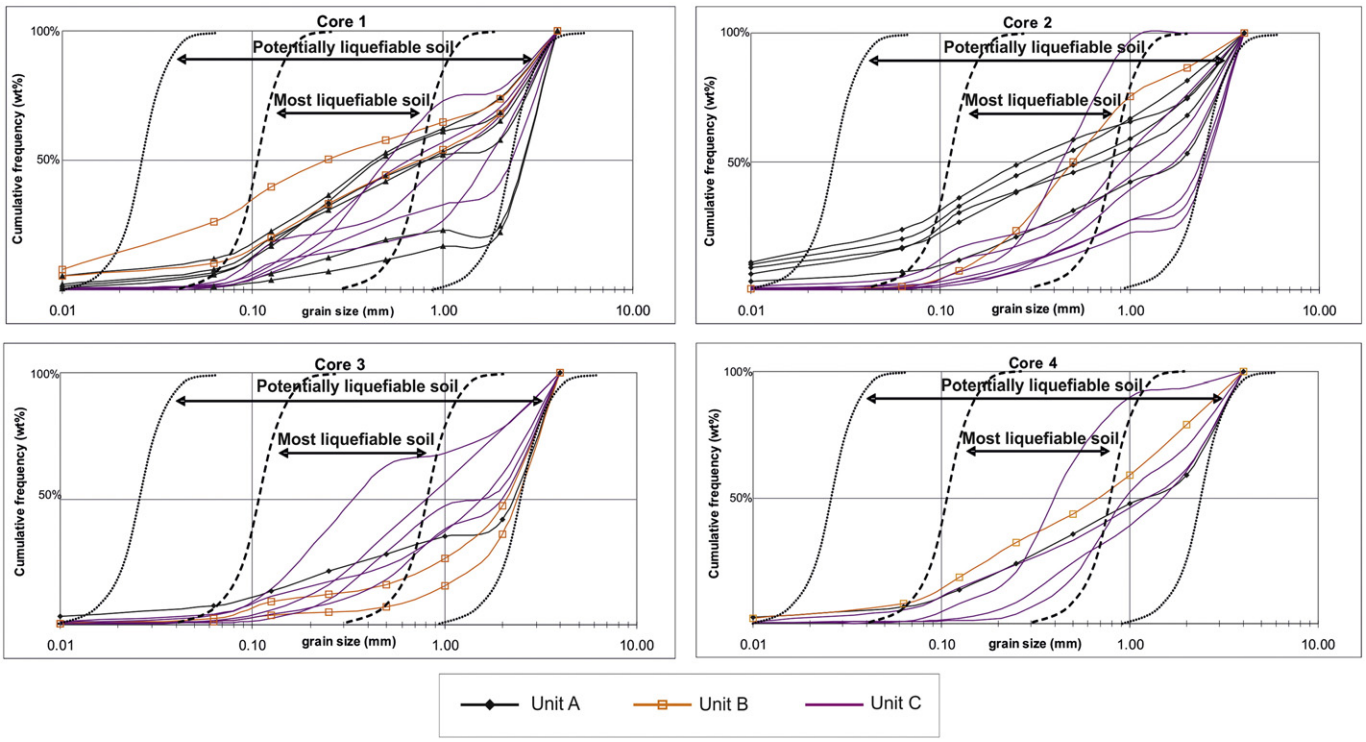

Fig. 13. The cumulative frequency curves for the Lechaion cores according to the units identified. All samples are included in the liquefaction boundary curves of Tsuchida and Hayashi (1971).

limitation of this investigation besides the lack of sand boil ejecta samples is that the top layer in core 2 corresponds to an artificial fill layer while the top layer in core 4 corresponds to the preparation ground of the temple resulting in comparison of different layers. During upward transportation the liquefied sand gets enriched with sidewall material (Obermeier et al., 1993) and variations between the two samples were expected since core 4 does not include artificial fill deposits. Therefore, the investigation was limited to potential qualitative similarities and differences between these two samples and the top layer samples in cores 1 and 3.

The samples in cores 2 and 4 are characterised as polymodal very coarse, poorly sorted sand layers with D_{50} of −1.35 to −1 φ and primary mode of −2 to 0 respectively. In contrast, core 1 and 3 samples are characterised as unimodal very fine gravel to very coarse sand that are poorly sorted with D_{50} of −2 φ and mode of −2 φ (Fig. 17). The characteristic mode of 0.75 φ has been identified only as a secondary mode in the sample of core 4 while it is absent from the rest of the samples.

The top layer samples do not correlate well with the rest of the potential liquefied sand layers and do not appear finer grained in relation to the intermediate and deeper sediments as suggested by Obermeier et al. (1993) and Cao et al. (2011). On the contrary, they appear coarser (Fig. 16). The first observation may be attributed to the mixing of the liquefied sediment with sidewall material. Since the sidewall material was coarser grained the top layers potentially could appear coarser than the original sand that liquefied. The second observation could be attributed to the impermeable mortar layer of the floor. This layer could have allowed sand finer than −1 φ and water to be ejected on the floor surface through small cracks but could have prevented grain sizes coarser than −1 φ moving in to the surface. However, it is interesting to note that the median D_{50} in the cores varies from −2.174 to 1.517 φ with coarser values in cores 1 and 3 and finer values in cores 2 and 4.

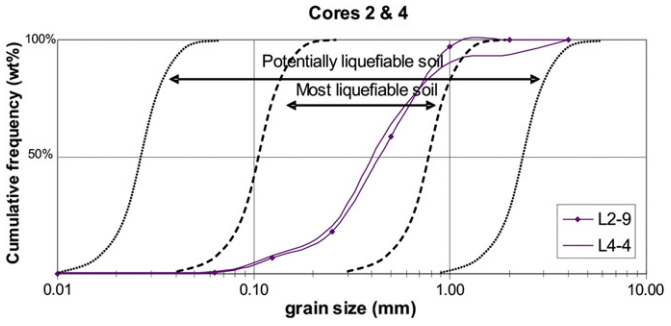

Fig. 14. The cumulative frequency diagrams from samples L2-9 and L4-4 that exhibit close parallelism and represent the most liquefiable deposits of the cores.

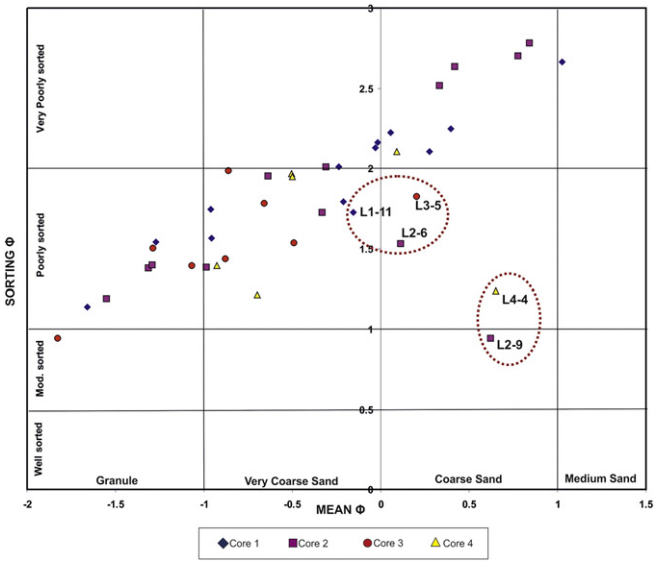

Fig. 15. Plot of sorting vs. mean grain size values for all samples from the cores. Dotted circles indicate sediments with high and relatively high potential of liquefaction.

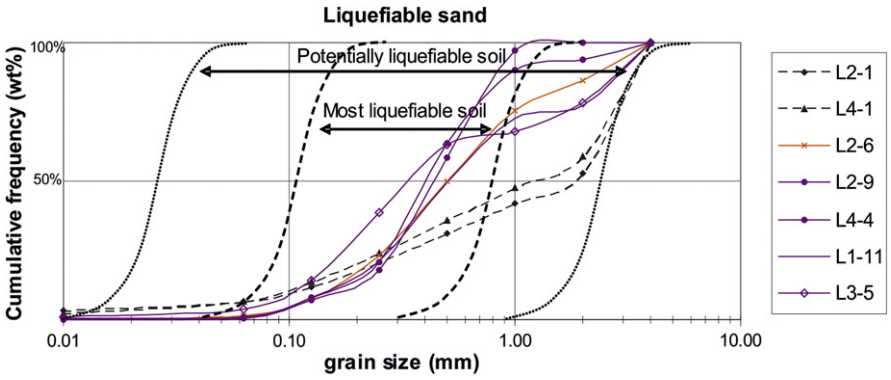

Fig. 16. Grain size distribution curves for all potential liquefied coarse sand samples in the four cores and the top layer samples in cores 2 and 4 (dashed grey lines).

This variation could be considered indicative of extensive mixing of vented sediment with sidewall material in cores 2 and 4 (Obermeier, 2009).

In summary, the grain size analysis indications that suggest a mixture of the top layers of cores 2 and 4 with liquefied ejected sand are the polymodality of the samples and their less coarse character in contrast to the unimodal and coarser sediments of the top layer samples in cores 1 and 3. Further indications of sediment mixing come from the median D_{50} values for the cores, where cores 2 and 4 appear finer than cores 1 and 3. Nevertheless, these observations are considered as rather weak. In lack of sand boil ejecta samples and given the potential implications that could be attributed to the mixing of the liquefied sand with variant sidewall material and the unclear role of the mortar floor base, no further study was considered necessary.

4. Synthesis and discussion

Investigations of the Early Christian Basilica using geomorphological, archaeological, geophysical and sedimentological methods provide information that allows us to suggest that the decorated floor of the Basilica preserves the geomorphic expressions of co-seismic features related to ground liquefaction.

4.1. Geomorphology—lithostratigraphy

The location of the temple on an estuarine sand bar separating the coast from the inner harbour represents a geomorphological setting susceptible to liquefaction (Kotoda et al., 1988; Youd and Perkins, 1978). The deposits are characterised by intercalations of layers of coarse silty sand to very coarse-grained sand and gravel with pebbles of up to 2–3 cm diameter. According to archaeological findings, the upper 1 m of the deposits represent artificial fill used to level the ground enabling the construction of the Basilica. The artificial nature of the upper 1 m is also indicated by the stratigraphy from cores 1 and 2 with layers that contain up to 10% clay and bear strong analogies to the archaeological stratigraphy. The absence of artificial fill deposits from cores 3 and 4 suggests that artificial fill was applied mainly in the central and WSW part of the temple indicating through an unconformity, a "palaeosurface", before the construction of the Basilica, dipping gently towards the WSW. The distribution of the artificial fill is also supported by the geophysical EM maps at 1.5 m depth suggesting more fine-grained permeable deposits to the WSW parts of the temple and coarser less permeable deposits to the ENE (Apostolopoulos et al., 2013).

The stratigraphy below the "palaeosurface" represented by Units B and C is characterised by coarse to very coarse sand and gravel with pebbles with minimal content of fines. It is not clear if the stratigraphy represents natural deposits since archaeological findings suggest that artificial fill deposits potentially extend down to a depth of 3 m (archaeological trial trenches 5 and 6). The EM map of 3 m depth is indicative of linear resistive zones running parallel to the central and northern aisle of the Basilica that potentially represent ancient harbour constructions that pre-date the Early Christian Basilica. These constructions due to their linear character and their orientation near parallel to the coastline and inner harbour shoreline could represent retaining walls related to harbour installations, indicating that the overlying sediments could be considered with caution as artificial.

The systematic use of the site as a harbour and the sediment mixing that occurred due to extensive dredging activities (Morhange et al., 2012; Pallas, 1965; Rothaus, 1995) does not allow a direct correlation of the deposits with natural coastal or fluvial processes, although potential short periods of abandonment could be responsible for their redeposition. Since archaeological investigations in the ancient Lechaion harbour are limited only to surface surveys, interpretations based on sedimentary deposits should be handled with care until archaeological excavations provide the necessary background information for site use and evolution.

4.2. Earthquake induced ground liquefaction

The initial indications for earthquake induced ground liquefaction came from the morphology of the surface structures that have caused

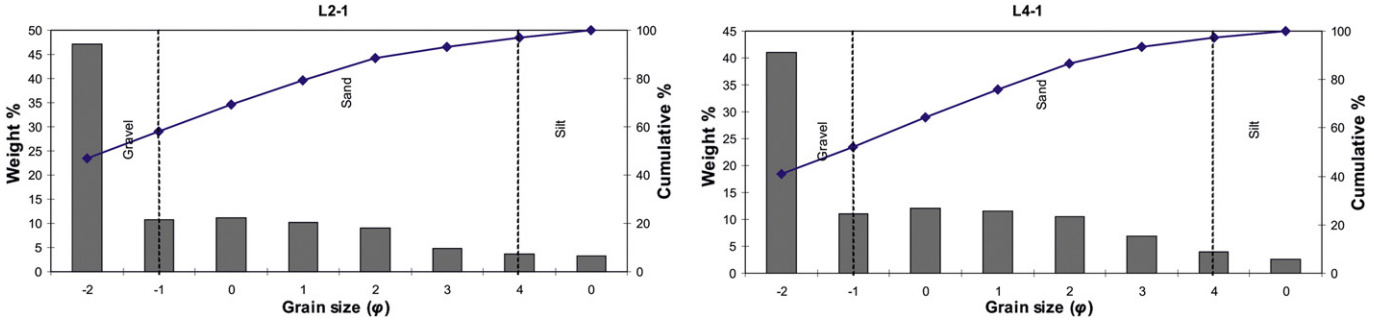

Fig. 17. Grain size histograms and cumulative frequency curves of top layers in cores 2 and 4.

extensive damages to the Basilica floor via linear and circular depressions and buckling structures These deformations correlate well with the surface expression of earthquake induced ground liquefaction of granular deposits (Obermeier, 2009; Tokimatsu and Seed, 1987), exhibiting a widespread distribution with a primary ENE–WSW trend and a secondary NNW–SSE trend.

The geophysical survey provided further indications for earthquake induced ground liquefaction processes suggesting extensive lateral spreading zones that develop in trends that correlate satisfactorily with the two trends recorded on the Basilica floor and with the local topographic setting, a predominant controlling factor for lateral spread orientation (Obermeier, 2009; Youd, 1984a). The survey suggests primary extensional displacement towards the free face of the inner harbour shore located down-slope to the SSE of the temple, manifested through near vertical fissure zones with an ENE–WSW strike. These primary lateral spreading zones are supported by both the EM second derivative of apparent conductivity map for 3 m effective depth range and the ERT LR-2 profile. These observations are not supported by the GPR survey since the profiles run parallel to the strike of the zones. The secondary lateral spread trend is expressed through near vertical fissure zones striking NNW–SSE that develop at right angles to the primary zones trend. The potential relationship of the secondary zones in relation to the primary zones is not clear and they have either developed independently towards a topographic low located to the WSW of the Basilica or potentially represent secondary structures accommodating the primary fissure zones displacements. These secondary lateral spreading zones are supported by moderate values in the EM second derivative of apparent conductivity map for 3 m effective depth range, in the ERT profile LR-1 and the GPR sections.

Lateral spreading as indicated by the ERT profiles, was triggered along a shear zone located at approximately 4 to 5 m depth. This shear zone represents the liquefied horizon that through cyclic shear stress, induced hydraulic fracturing on the overlying strata and rapid upward drainage of the saturated deposits through extensional fissures, creating blocks that were transported downslope (Andrus, 1986; Bartlett and Youd, 1992; Obermeier et al., 2005; Rodríguez-Pascua et al., 2015; Youd, 1984a). The substratum horizontal displacement is estimated to several meters since the separation of the overlying blocks ranges from 0.5 to 2 m. Vertical displacement of the order of 1 m is suggested by the LR-2 resistivity section.

Grain size analysis of the sedimentary samples from the four vibracores identified sand layers exhibiting high liquefaction potential. These layers were recorded in Unit C in cores 2 and 4 positioned in the circular depressions. Additional potential liquefaction sand layers were identified in Unit C and in Unit B. The stratigraphic location and depth distribution of the high liquefaction potential layers in Unit C indicate a liquefaction sediment source horizon below 4 m that is in agreement with the geophysical survey results.

Potential correlation of the deformation structures observed with ground failure mechanisms relating to flood induced seepage produced by potential variations in hydraulic head differences between the inner harbour basin and the coastline expressed through piping and sand boils, was examined according to observations and criteria proposed by Li et al. (1996). The planar morphology and lateral distribution of the conduits suggest violent and episodic vertical displacements of the substratum, related to sudden and violent increase of the pore water pressure in the liquefied horizon through cyclic shear waves, leading to hydraulic fracturing of the overlying stratum (Obermeier, 2009; Rodríguez-Pascua et al., 2015). This hydraulic fracturing develops along lateral spreading zones, expressed through the surface depressions and buckling structures. Therefore, the ground deformation observed on the floor and the substratum of the Basilica clearly supports seismic shear stress deformation through ground liquefaction (Li et al., 1996; Obermeier, 2009; Owen and Moretti, 2011; Rodríguez-Pascua et al., 2015).

4.3. Indications for recurrence of liquefaction

The Basilica construction, although it preserves liquefaction deformation structures on its floor, does not present horizontal and vertical displacements of the extent suggested by the lateral spreading as depicted in the geophysical survey. This observation suggests that the substratum deformation observed represents the cumulative effect of a number of liquefaction events, indicating recurrence of liquefaction (Andrus, 1986; Obermeier, 2009; Youd, 1984b). The liquefaction sand samples located in Units C and B under the unconformity expressing a "palaeosurface" indicate that liquefaction and initial opening of fissures pre-dates the construction of the Basilica. Therefore it can be suggested that at least one earthquake induced liquefaction event occurred on the site before the construction of the Basilica, potentially during the use of the harbour during antiquity (Fig. 18).

This event involved Unit C of the substratum. Although the unit is characterised by minimal content of fines, it behaved as an impermeable cap triggering hydraulic pressure rise and liquefaction of the underlying fine-grained sand deposits. The impermeable behaviour of Unit C could be attributed to dense packing. Although natural processes cannot be ruled out, the dense packing could relate to artificial fill deposits. Unit B potentially represent a period of gradual filling of the lateral spread surface cracks as suggested by the clay rich intercalations recorded in core 1. Again it is not known if this filling is natural or artificial. The Unit B layer in core 2 with a high liquefaction potential (L2-6) might indicate ejected sand deposit of this event corresponding to an *event horizon*.

When the Early Christian Basilica was founded, Unit A was gradually laid down on the existing "palaeosurface", with artificial fill deposits concentrated mainly in the WSW part of the temple for the levelling of the ground that was gently dipping towards the WSW. It is not clear if this gentle dip was the result of the liquefaction lateral spreading of the <5th c. A.D. seismic event(s) or if it pre-existed.

After the construction of the Basilica, recurrence indications of at least one liquefaction event is suggested that potentially relate to its destruction by the earthquake of A.D. 551. This is inferred from the good correlation between the majority of the surface deformation structures and the lateral spreading zones identified in the geophysical survey suggesting reactivation of the lateral spreading trends. This reactivation is expressed through the widespread deformation of the temple floor and localised settlement of the order of 0.34 m of the preparation ground horizon and overlying artificial fill as suggested by the core stratigraphy. However, ejected sand from this event is absent since it was ejected on to the floor of the temple and any traces were removed during archaeological excavation and recent restoration works. The only weak indication of ejected sand comes from the top layers in cores 2 and 4 that appear finer compared to the top layers of cores 1 and 3.

Indications for a potential third liquefaction event that post-dates the construction of the Basilica and possibly pre-dates the A.D. 551 earthquake comes from the northern aisle of the temple. In the NW part of the aisle a circular depression with dimensions 1.48 × 2.5 m and 0.3 m depth, preserves remains of an earlier floor surface, including tiles and mortar, located 0.20 m under the surface of the Basilica floor (Fig. 19). These remains, give the impression that they belong to the same period as the Basilica since it is composed of similar tiles and mortar, potentially representing an earlier construction phase (D. Athanasoulis, personal communication, 2013).

The remains suggest that the floor of the northern aisle at some point underwent restoration. The extent of this restoration is unknown but observations indicate that it was applied throughout the northern aisle. These observations include: (i) the location of the northern aisle floor exactly 0.20 m higher than the central and the southern aisles of the temple (Pallas, 1960) and (ii) the variance in the north aisle floor decoration that according to Pallas (1959) "*appears less elaborated*" compared to the southern aisle. These observations suggest that the remains potentially represent the original floor of the northern aisle

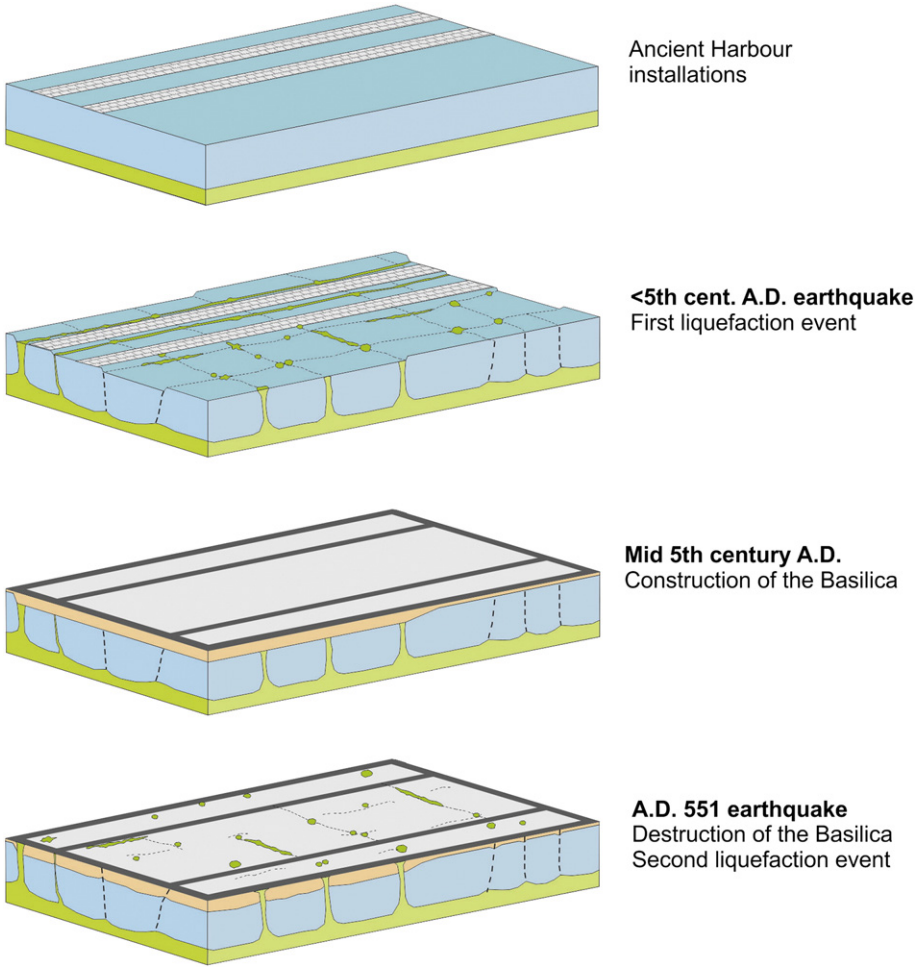

Fig. 18. Schematic representation of the substratum evolution of the site from antiquity till A.D. 550 through the manifestation of at least two earthquake induced liquefaction events.

that at a later phase it was restored with the tiling of a later floor surface. The location of the earlier floor remains at the margins of the depression suggest that both floors were damaged by the same process, i.e. the recurrence of ground liquefaction through the reactivation of pre-existing sand vents resulting to localised settlements (Obermeier, 2009, and references therein). Therefore, a third potential seismic event is suggested to have induced ground liquefaction, before the A.D. 551 event.

Summarizing, potential indications for ground liquefaction recurrence suggest at least three liquefaction events. Indications for the potential event(s) pre-dating the construction of the Basilica are suggested mainly by the comparison of the geophysical survey results with the field observations supported by the lithostratigraphy. The second event, relates to the severe damages the temple suffered during the A.D. 551 event, through the good correlation of the surface structures trends with the lateral spreading zones suggested by the geophysical survey. Finally, a potential third liquefaction event is suggested by archaeological indications and earlier floor remains in the margins of a circular depression, during an earthquake post-dating the construction of the Basilica and pre-dating the destruction of the temple by the A.D. 551 event.

Fig. 19. The remains of an earlier floor surface under the Basilica floor in the margins of a circular depression in the northern aisle.

4.4. Potential relative dates of the events

Due to the localised nature of the study in a region characterised by intense seismic activity, the identification of potential seismogenic sources that could relate to these events is a challenging task (Caputo and Helly, 2008). Nevertheless, a preliminary examination of the historical record according to Papazachos and Papazachou (1989), provides indications for the candidate periods/dates that could relate to these events.

Historical accounts by Procopius, Caesarea and others locate the earthquake of A.D. 551 in the broader region of Phokida and describe it as a disastrous earthquake ($M_L = 7.2$) with a macroseismic MMI of IX, responsible for the destruction of numerous villages and cities in Boiotia, Achaia and the Gulf of Itea (Papazachos and Papazachou, 1989). Although Ancient Corinth is not mentioned to have suffered damages, archaeological excavations in the region suggest that Corinth was one of the cities affected by the earthquake of A.D. 551 (Papazachos and Papazachou, 1989, and references therein).

The surface deformation structures on the floor of the Early Christian Basilica provide a sense of extensive and severe liquefaction effects from

a strong seismic event. Archaeological findings and stratigraphic successions of archaeological deposits overlying the Early Christian Basilica floor suggest that the earthquake in A.D. 551 caused severe irreparable damages leading to the gradual destruction of the monument (Pallas, 1959, 1960, 1965). This gradual destruction of the temple included initial collapse of the roof ceramic tiles and mortar from the walls followed by the looting of the main structural elements of the temple such as pillars and masonry blocks. This suggestion is supported by the stratigraphy overlying the temple floor that indicates a packed layer of variable thickness throughout the temple composed of fragments of ceramic tiles and mortar located between the floor surface and the limited structural elements of the Basilica preserved (Pallas, 1956, 1960, 1957). This archaeological layer, besides being indicative for the gradual destruction of the monument, is also indicative of the limited potential for impact block marks from structural elements that could have contributed to the extensive deformation structures observed on the floor. The gradual destruction of the temple is further supported by archaeological findings (Pallas, 1957, Pallas, 1960) suggesting use of the temple's sanctum till the end of the 11th century A.D.

The potential third ground liquefaction event pre-dating the A.D. 551 earthquake, correlates well with the A.D. 524 event that occurred during the reign of Ioustin A′ (A.D. 518–527). The epicentre is estimated to 8 km ($M_L = 6.6$) distance from the Early Christian Basilica with a macroseismic MMI of IX for Ancient Corinth (Papazachos and Papazachou, 1989). According to the historical record of Malalas, Theofanis, Cedren, Procopius and others, the earthquake destroyed Ancient Corinth and surrounding towns and reconstructions were carried out under the order of Emperor Ioustin A′(Papazachos and Papazachou, 1989). Archaeological records suggest potential construction works during the reign of Ioustin A′ (A.D. 518–527). The restoration character of these works is suggested by the floor remains as observed in the margins of a sand vent (Fig. 19). Supplementary construction works located to the west and the south of the temple (Pallas, 1959) as suggested through depressions filled with rubble of wall plaster and marble, dated to the 3rd decade of the 6th century A.D. and not earlier than A.D. 518 according to coins of Ioustin A′ (Pallas, 1959), indicate a general reconstruction of the temple. Finally, the stratigraphic and the chronological discontinuity as described by Pallas (1965) in trial trench 2 (Fig. 7), is also indicative of damaged floor and potential restoration works through the vertical discontinuity in the artificial fill deposits. These deposits date to the same period (A.D. 518–527) as the depressions in the west and south of the temple. Therefore, a third seismic event that induced ground liquefaction to the site is suggested by potential restoration works during the reign of Ioustin A′.

According to Rodríguez-Pascua et al. (2011), restoration works represent an indirect Earthquake Archeological Effect. Since the proposed archaeological dating for these works is in good correlation with the seismic event of A.D. 524, it can be suggested that the earthquake of A.D. 524 induced ground liquefaction to the site, through the reactivation of pre-existing sand vents (Fig. 19), that caused repairable damages to the temple as indicated by the stratigraphic discontinuity in trench 2 and the preservation of earlier floor remains in a circular depression. Nevertheless, these observations are indirectly indicative and they should be correlated with future archaeological investigations in the Early Christian Basilica.

The earthquake event(s) that potentially relate to the liquefaction event(s) that pre-date the construction of the Basilica, based strictly on historical accounts can be no other but the earthquake in A.D. 77 ($M_L = 6.3$), an event with macroseismic MMI of IX, located at 4 km distance from the ancient harbour (Papazachos and Papazachou, 1989). Described by Malalas, the event caused extensive damage to the ancient city of Corinth and aid was provided by the Roman Emperor Vespasian (Papazachos and Papazachou, 1989). However, two periods of harbour reconstructions have been suggested during the Roman period, the first during A.D. 40–45 during the Roman colonization of Corinth and a second during the years A.D. 353–358 according to an inscription found in the harbour (Rothaus, 1995; Stiros et al., 1996 and references therein). Although the motives for these reconstructions are not known, they potentialy represent indirect indications of seismic events of the period (Rodríguez-Pascua et al., 2011). Finally, a seismic event that triggered subsidence at Kenchreai harbour during the early 5th century A.D. (Rothaus, 1995), could also potentially associate with the liquefaction event in Lechaion harbour.

Further potential indications of historical periods that could relate to these events come from earth science studies based on earthquake environmental effects. Geoarchaeological studies in the ancient harbour suggest an episodic seismic uplift event of the order of 1.10 m before the Roman colonization (44 B.C.), dated to 500–200 B.C. (Stiros et al., 1996). The implication is that the total uplift recorded in the harbour could be associated with a series of seismic events rather than a single earthquake (Morhange et al., 2012; Stiros et al., 1996; Turner et al., 2010). Hadler et al. (2013), recalibrated radiocarbon dates from Stiros et al. (1996) and Morhange et al. (2012), suggesting a single co-seismic uplift and tsunami event during 146–44 B.C., again before the Roman colonization. In addition, Mourtzas et al. (2014) propose co-seismic submergence of the outer harbour moles by 1.60 m during A.D. 362–375, after the reconstruction of the harbour. Therefore, environmental effects from the ancient harbour are indicative of three candidate periods for the liquefaction event(s) that pre-date the construction of the Basilica.

Correlation of the two ground liquefaction events that affected the Basilica (A.D. 524 and A.D. 551) with the second submergence event (A.D. 522–580) of the order of 0.40 m as suggested by Mourtzas et al. (2014) and the tsunamigenic impact (6th c A.D.) as suggested by Hadler et al. (2013), potentially indicate a variety of earthquake environmental effects triggered by the same event(s), but further studies are required, in order to investigate this hypothesis.

Finally, ground liquefaction events relating to earthquake activity that post-date the destruction of the Early Christian Basilica in A.D. 551 as indicated by an uplift of the order of 1.10 m expressing the cumulating effect of seismic events (Mourtzas et al., 2014), potentially have contributed to an extent to the surface and substratum structures observed (Ambraseys, 2006; Rothaus et al., 2008), and require further investigations.

5. Conclusions

The study of ground deformation structures of the Early Christian Basilica has revealed that the site has suffered repeatedly from ground liquefaction induced by historical earthquake events. Through the study of archaeological records and their correlation with the geophysical survey results, the stratigraphy, and the historical records, at least two and potentially three ground liquefaction events are indicated. These indications, although they require further analysis, are indicative of (i) seismic event(s) that have caused considerable damage to the ancient harbour installations that pre-date the construction of the Basilica, (ii) severe but repairable damage to the Early Christian Basilica caused by the A.D. 524 event, followed by (iii) A.D. 551 earthquake, that caused severe and irreparable damages to the temple gradually leading to its collapse and abandonment.

Earthquake induced liquefaction is considered as an off-fault geological effect and according to its classification in the Earthquake Archaeological Effects (EAEs) as proposed by Rodríguez-Pascua et al. (2013) it correlates with minimum macroseismic EMS-98 and environmental ESI-07 intensity of VIII.

The damage classification for masonry buildings as suggested in the EMS-98 intensity scale (Grünthal, 1998), indicates very heavy damage (grade 4) for EMS-98 intensity of VIII, that is in agreement with the structural damage of the temple as suggested by the archaeological records. In addition, the ground deformation structures and features as recorded on the floor and the substratum of the Basilica are in good correlation with the Earthquake Environmental Effects suggested by

the ESI-07 scale for intensity VIII with sand boils up to ca. 1 m in diameter, ground settlements up to ca. 0.3 m, and localised lateral spreading with fissuring parallel to waterfront areas (Michetti et al., 2007). Subsequently, according to the results of this study, a minimum EMS-98 and ESI-07 intensity value of VIII can be suggested for the archaeological site of the Early Christian Basilica during the A.D. 551 earthquake.

The vicinity of the ancient harbour of Lechaion is indicative of a variety of earthquake environmental effects suggesting that the site represents an archaeological site with high potential value in earthquake science. Future archaeological excavations and further multidisciplinary studies in the vicinity of the ancient harbour will allow a better correlation of earthquake archaeological and environmental effects with potential seismogenic sources through empirical relationships and their associations, contributing to the regional historical seismicity catalogues and seismic hazard assessment.

Acknowledgments

We would like to thank D. Athanasoulis, Director of the 25th Ephorate of Byzantine Antiquities for allowing us to carry out the study at the site, and for the fruitful discussions and to express our deep gratitude to the Ephorate's personnel at the site for their warm support during our fieldwork. Additionally, many thanks to G. Amolochitis Geophysicist of NTUA Applied Geophysics Laboratory, A. Papadopoulos and A. Stylianou NTUA students for their assistance during the geophysical survey, and to D. Vandarakis, HUA research assistant, for assisting us in the vibracores drilling. Finally, cordial thanks to Fanis Chatoupis, geologist, for his geotechnical support, who helped us overcome unexpected obstacles during fieldwork. The research was conducted as part of Despina Minos-Minopoulos PhD thesis in the Department of Geography, Harokopio University, Athens, Greece.

References

Abu Zeid, N., Bignardi, S., Caputo, R., Santarato, G., Stefani, M., 2012. Electrical resistivity tomography of coseismic liquefaction and fracturing at San Carlo, Ferrara Province, Italy. Ann. Geophys. 55 (4), 713–716.

Allmendinger, R.W., Cardozo, N., Fisher, D., 2012. Structural Geology Algorithms: Vectors and Tensors in Structural Geology. Cambridge University Press 978-1107401389, p. 302.

Al-Shukri, H.J., Mahdi, H.H., Tuttle, M., 2006. Three-Dimensional Imaging of Earthquake-induced Liquefaction Features with Ground Penetrating Radar, Near Marianna. Arkansas. Seismol. Res. Lett. 77 (4), 505–513.

Ambraseys, N.N., 2006. Earthquakes and archaeology. J. Archaeol. Sci. 33, 1008–1016.

Andrus, R.D., 1986. Subsurface investigations on a liquefaction induced lateral spread, Thousand Springs Valley, Idaho: liquefaction recurrence and a case history in gravel (Master of Science Thesis) Department of Civil Engineering, Brigham Young University, p. 128.

Apostolopoulos, G., Minos-Minopoulos, D., Amolochitis, G., Pavlopoulos, K., Papadopoulos, A., 2013. Geophysical investigation for the detection of liquefaction phenomena in an archaeological site, Lechaion, Greece. Near surface Geoscience 2013—19th European Meeting of Environmental and Engineering Geophysics Bohum, Germany, 9–11 September 2013, TuS2b06.

Armijo, R., Meyer, B., King, G.C.P., Rigo, A., Papanastassiou, D., 1996. Quaternary evolution of the Corinth Rift and its implications for the Late Cenozoic evolution of the Aegean. Geophys. J. Int. 126, 11–53.

Audemard M., F.A., 2002. Soil liquefaction during the Caracas 1967 and Boca de Tocuyo 1989 earthquakes, Venezuela: its significance for human settlements on active alluvial areas and coastlands. In: Jackson, T.A. (Ed.), Caribbean Geology: Into the Third Millenium: Transactions of the Fifteenth Caribbean Geological Conference, chapter 21, pp. 229–234.

Audemard M., F.A., Michetti, A.M., 2011. Geological criteria for evaluating seismicity revisited: forty years of paleoseismic investigations and the natural record of past earthquakes. Geol. Soc. Am. Spec. Pap. 479, 1–21.

Barnes, G.L., 2010. Earthquake archaeology in Japan: an overview. In: Sintubin, M., Stewart, I.S., Niemi, T.M., Altunel, E. (Eds.), Ancient Earthquakes. Geological Society of America Special Paper 471. http://dx.doi.org/10.1130/2010.2471(08).

Bartlett, S.F., Youd, T.L., 1992. Empirical analysis of horizontal ground displacement generated by liquefaction-induced lateral spreads. Technical Report NCEER-92-0021. National Centre for Earthquake Engineering Research, New York, p. 126.

Blott, S.J., Pye, K., 2001. Gradistat: a grain size distribution and statistics package for the analysis of unconsolidated sediments. Earth Surf. Processes Landforms 26, 1237–1248.

Cao, Z., Youd, L.T., Yuan, X., 2011. Gravelly soils that liquefied during 2008 Wenchuan, China earthquake, Ms = 8.0. Soil Dyn. Earthq. Eng. 31, 1132–1143.

Caputo, R., Helly, B., 2008. The use of distinct disciplines to investigate past earthquakes. Tectonophysics 453, 7–19.

Charalampakis, M., Lykousis, V., Sakellariou, D., Papatheodorou, G., Ferentinos, G., 2014. The tectono-sedimentary evolution of the Lechaion Gulf, the south eastern branch of the Corinth graben, Greece. Mar. Geol. 351, 58–75.

Coulter, H.W., Ralph, R.M., 1966. Effects of the Earthquake of March 27, 1964 at Valdez, Alaska. U.S. The Alaska Earthquake, March 27, 1964, Effects on Communities. Geological Survey Professional Paper 542-C (Washington).

Curray, J.R., 1960. Tracing sediment masses by grain size modes. 21st Intern. Geological Congress, Norden, Proc. Pt. 23, pp. 119–130.

Flemming, N.C., 1978. Holocene Eustatic changes and coastal tectonics in the Northeast Mediterranean: implications for models of crustal consumption. Philos. Trans. R. Soc. Lond. A 289, 405–458.

Friedman, G.M., 1967. Dynamic processes and statistical parameters compared for size frequency distribution of beach and river sands. J. Sediment. Petrol. 37 (2), 327–354.

Folk, R.L., Ward, W.C., 1957. Brazos River Bar: a study in the significance of grain size parameters. J. Sediment. Petrol. 27 (1), 3–26.

Galli, P., 2000. New empirical relationships between magnitude and distance for liquefaction. Tectonophysics 324, 169–187.

Grünthal, G. (Ed.), 1998. European Macroseismic Scale 1998: EMS-98. Musée National d'Historie Narurelle (Luxembourg, 99 pp.).

Hadler, H., Vött, A., Koster, B., Mathes-Schmidt, M., Mattern, T., Ntageretzis, K., Reicherter, K., Sakellariou, D., Willershäuser, T., 2011. Lechaion, the ancient harbour of Corinth (Peloponnese, Greece) destroyed by tsunamigenic impact. Proceedings of the 2nd INQUA-IGCP-467 International Workshop on Active Tectonics, Earthquake Geology, Archaeology and Engineeering, Corinth Greece 2011.

Hadler, H., Vött, A., Koster, B., Mathes-Schmidt, M., Mattern, T., Ntageretzis, K., Reicherter, K., Willershäuser, T., 2013. Multiple late-Holocene Tsunami Landfall in the Eastern Gulf of Corinth Recorded in the Palaeotsunami Geo-archive at Lechaion, Harbour of Ancient Corinth (Peloponnese, Greece). Z. Geomorphol. 57 (4), 139–180.

Inoue, T., Kimura, K., Miyachi, Y., Haraguchi, T., Tanabe, S., Inouchi, Y., 2006. Identification of the source horizon of earthquake-jetted sand based on grain size characteristics and sand fraction composition. Earth Sci. 60, 315–324.

Kanaori, Y., Kawakami, S., Yairi, K., Hattori, T., 1993. Liquefaction and flowage at archaeological sites in the inner belt of central Japan: tectonic and hazard implications. Eng. Geol. 35, 65–80.

Karakhanyan, A., Avagyan, A., Sourouzian, H., 2010. Archaeoseismological studies at the temple of Amenhotep III, Luxor, Egypt. In: Sintubin, M., Stewart, I.S., Niemi, T.M., Altunel, E. (Eds.), Ancient Earthquakes. Geological Society of America Special Paper 471. http://dx.doi.org/10.1130/2010.2471(17).

Keraudren, B., Sorel, D., 1987. The terraces of Corinth (Greece). A detailed record of eustatic sea-level variations during the last 500.000 years. Mar. Geol. 77, 99–107.

Koster, B., Reicherter, K., Vött, A., Grützner, C., 2011. The evidence of tsunami deposits in the gulf of Corinth (Greece) with geophysical methods for spatial distribution. Proceedings of the 2nd INQUA-IGCP-467 International Workshop on Active Tectonics, Earthquake Geology, Archaeology and Engineeering, Corinth Greece 2011.

Kotoda, K., Wakamatsu, K., Masahiko, O., 1988. Mapping liquefaction potential based on geomorphological land classification. Proceedings of Ninth World Conference on Earthquake Engineering, August 2–9, 1988, Tokyo, Japan, III, pp. 195–200.

Leeder, M.R., McNeill, L.C., Collier, R.E.L.L., Portman, C., Rowe, P.J., Andrews, J.E., Gawthorpe, R.L., 2003. Corinth rift margin uplift: new evidence from Late Quaternary marine shorelines. Geophys. Res. Lett. 30 (12), 13.1–13.4.

Leeder, M.R., Portman, C., Andrews, J.E., Collier, R.E.L.L., Finch, E., Gawthorpe, L.C., McNeill, L.C., Perez-Arlucea, M., Rowe, P., 2005. Normal faulting and crustal deformation, Alkyonides Gulf and Perachora peninsula, eastern Gulf of Corinth rift, Greece. J. Geol. Soc. Lond. 162, 549–561.

Li, Y., Craven, J., Schweig, E.S., Obermeier, S.F., 1996. Sand boils induced by the 1993 Mississippi River flood: could they one day be misinterpreted as earthquake-induced liquefaction? Geology 24 (2), 171–174.

Liu, L., Li, Y., 2001. Identification of liquefaction and deformation features using ground penetrating radar in the New Madrid seismic zone, USA. J. Appl. Geophys. 47, 199–215.

Mariolakos, I., Stiros, S.C., 1987. Quaternary deformation of the Isthmus and Gulf of Corinthos (Greece). Geology 15, 225–228.

Maurya, D.M., Goyal, B., Patidar, A.K., Mulchandani, N., Thakkar, M.G., Chamyal, L.S., 2006. Ground Penetrating Radar imaging of two large sand blow craters related to the 2001 Bhuj earthquake, Kachchh, Western India. J. Appl. Geophys. 60, 142–152.

Michetti, A.M., Esposito, E., Guerrieri, L., Porfido, S., Serva, L., Tatevossian, R., Vittori, E., Audemard, F., Azuma, T., Clague, J., Comerci, V., Gurpinar, A., McCaplin, J., Mohammadioun, B., Mörner, N.A., Ota, Y., Roghozin, E., 2007. Intensity Scale ESI 2007. In: Guerrieri, L., Vittori, E. (Eds.), Mem. Descr. Carta Geol. d'Italia vol. 74. Servizio Geologico d'Italia-Dipartimento Difesa del Suolo, APAT, Rome, Italy.

Morhange, C., Pirazzoli, P.A., Evelpidou, N., Marriner, N., 2012. Late Holocene tectonic uplift and the silting up of Lechaion, the Western Harbor of Ancient Corinth, Greece. Geoarchaeol. Int. J. Short Commun. 27, 278–283.

Mourtzas, N.D., Kissas, C., Kolaiti, E., 2014. Archaeological and geomorphological indicators of the historical sea level changes and the related palaeogeographical reconstruction of the ancient foreharbour of Lechaion, East Corinth Gulf (Greece). Quat. Int. 332, 151–171.

Obermeier, S.F., 1996. Use of liquefaction-induced features for paleoseismic analysis—An overview of how seismic liquefaction features can be distinguished from other features and how their regional distribution and properties of source sediment can be used to infer the location and strength of Holocene paleo-earthquakes. Eng. Geol. 44, 1–76.

Obermeier, S.F., 2009. Using Liquefaction-induced and other soft-sediment features for paleoseismic analysis 2009 In: McCaplin, J. (Ed.), Paleoseismology. International Geophysics 95. http://dx.doi.org/10.1016/S0074-6142(09)95007-0.
Obermeier, S.F., Pond, E.C., 1999. Issues in using liquefaction features for paleoseismic analysis. Seismol. Res. Lett. 70 (1), 34–58.
Obermeier, S.F., Martin, J.R., Frankel, A.D., Youd, T.L., Munson, P.J., Munson, C.A., Pond, E.C., 1993. Liquefaction evidence for one or more strong Holocene earthquakes in the Wabash Valley of southern Indiana and Illinois, with preliminary estimate of magnitude. U. S. Geol. Surv. Prof. Pap. 1536.
Obermeier, S.F., Olson, S.M., Green, R.A., 2005. Field occurrences of liquefaction-induced features: a primer for engineering geological analysis of paleoseismic shaking. Eng. Geol. 76, 209–234.
Owen, G., Moretti, M., 2011. Identifying triggers for liquefaction-induced soft-sediment deformations in sands. Sediment. Geol. 235, 141–147.
Pallas, D.I., 1956. Lechaion Basilica Excavation. Proceedings of the Archaeological Society at Athens, (1961), pp. 164–178 (in Greek).
Pallas, D.I., 1957. Lechaion Basilica Excavation. Proceedings of the Archaeological Society at Athens, (1962), pp. 95–104 (in Greek).
Pallas, D.I., 1959. Lechaion Basilica Excavation. Proceedings of the Archaeological Society at Athens, (1965), pp. 126–140 (in Greek).
Pallas, D.I., 1960. Lechaion Basilica Excavation. Proceedings of the Archaeological Society at Athens, (1966), pp. 144–170 (in Greek).
Pallas, D.I., 1965. Lechaion Basilica Excavation. Proceedings of the Archaeological Society at Athens, (1967), pp. 137–166 (in Greek).
Papathanassiou, G., Pavlides, S., Christaras, B., Pitilakis, K., 2005. Liquefaction case histories and empirical relations of earthquake magnitude versus distance from the broader Aegean region. J. Geodyn. 40, 257–278.
Papazachos, B., Papazachou, K. (Eds.), 1989. The Earthquakes of Greece. Ziti Publications, Thessaloniki, p. 356 (1999, in Greek).
Pavlides, S., Caputo, R., 2004. Magnitude versus faults' surface parameters: quantitative relationships from the Aegean Region. Tectonophysics 380, 159–188.
Pirazzoli, P.A., Stiros, S.C., Arnold, M., Laborel, J., Laborel-Deguen, F., Papageorgiou, S., 1994. Episodic uplift deduced from Holocene shorelines in the Perachora Peninsula, Corinth area, Greece. Tectonophysics 229, 201–209.
Rodríguez-Pascua, M.A., Garduño-Monroy, V.H., Israde-Alcántara, I., Pérez-López, R., 2010. Estimation of the paleoepicentral area from the spatial gradient of deformation in lacustrine seismites (Tierras Blancas Basin, Mexico). Quat. Int. 219, 66–78.
Rodríguez-Pascua, M.A., Pérez-López, R., Giner-Robles, J.L., Silva, P.G., Garduño-Monroy, V.H., Reicherter, K., 2011. A comprehensive classification of Earthquake Archaeological Effects (EAE) in archaeoseismology: application to ancient remains of Roman and Mesoamerical cultures. Quat. Int. 242, 20–30.
Rodríguez-Pascua, M.A., Silva, P.G., Pérez-López, R., Giner-Robles, J.L., Martín-González, F., Perucha, M.A., 2013. Preliminary intensity correlation between macroseismic scales (ESI07 and EMS98) and Earthquake archaeological effects (EAEs). Proceedings of the 4th International INQUA Meeting on Paleoseismology, Active Tectonics and Archeoseismology (PATA), 9–14 October 2013, Aachen, Germany.
Rodríguez-Pascua, M.A., Silva, P.G., Pérez-López, R., Giner-Robles, J.L., Martín-González, F., Del Moral, B., 2015. Polygenetic sand volcanoes: on the features of liquefaction processes generated by a single event (2012 Emilia Romagna 5.9 M_w earthquake, Italy. Quat. Int. 357, 329–335.
Rothaus, R., 1995. Lechaion, western port of Corinth: a preliminary archaeology and history. Oxf. J. Archaeol. 14 (3), 293–306.
Rothaus, R., Reinhardt, E.G., Noller, J.S., 2008. Earthquakes and subsidence at Kenchreai: using recent earthquakes to reconsider the archaeological and literary evidence. In: Hall, L.J., Caraher, W., Moore, R.C. (Eds.), Archaeology and History in Roman, Medieval and Post-Medieval Greece. Ashgate Publishing Ltd, p. 351.
Sakellariou, D., Fountoulis, I., Lykousis, V., 2004. Lechaion Gulf: the last descendant of the Proto-Gulf-of-Corinth basin. Proceedings of the 5th International Symposium on Eastern Mediterranean Geology, Thessaloniki, Greece, 14–20 April 2004. 2, pp. 881–884.
Sakellariou, D., Lykousis, V., Alexandri, S., Kaberi, H., Rousakis, G., Nomikou, P., Georgiou, P., Ballas, D., 2007. Faulting, seismic-stratigraphic architecture and Late Quaternary evolution of the Gulf of Alkyonides Basin—East Gulf of Corinth, Central Greece. Basin Res. 19, 273–295.
Sangawa, A., 2009. A study of paleoearthquakes at archaeological sites—A new interdisciplinary area between paleoseismology and archaeology. Translation from. Synthesiology 2 (2), 91–100.
Scranton, R.L. (Ed.), 1957. Mediaeval Architecture: In the Central Area of Corinth vol. 16. The American School of Classical Studies at Athens, Princeton N.J., p. 147.
Stiros, S., Pirazzoli, P., Rothaus, R., Papageorgiou, S., Laborel, J., Arnold, M., 1996. On the date of construction of Lechaion, Western Harbour of Ancient Corinth, Greece. Geoarchaeol. Int. J. 11 (3), 251–263.
Takahama, N., Otsuka, T., Brahmantyo, B., 2000. A new phenomenon in ancient liquefaction—the draw-in process, its final stage. Sediment. Geol. 135, 157–165.
Tokimatsu, K., Seed, B., 1987. Evaluation of settlements in sands due to earthquake shaking. J. Geotech. Eng. 113 (8), 861–878.
Tsuchida, H., Hayashi, S., 1971. Estimation of liquefaction potential of sandy soils. Proceedings of the 3rd Joint Meeting, U.S.–Japan Panel on Wind and Seismic Effects. U.S.–Japan Cooperation Program (UNJR), Tokyo, pp. 91–101.
Turner, J.A., Leeder, M.r., Andrews, J.E., Rowe, P.J., Van Calsteren, P., Thomas, L., 2010. Testing rival tectonic uplift models for the Lechaion Gulf in the Gulf of Corinth rift. J. Geol. Soc. Lond. 167, 1237–1250.
Tuttle, M., Lafferty III, R.H., Cande, R.F., Sierzchula, M.C., 2011. Impact of earthquake-induced liquefaction and related ground failure on a Mississippian archaeological site in the New Madrid seismic zone, central USA. Quat. Int. 242, 126–137.
Vita-Finzi, C., King, G.C.P., 1985. The seismicity, geomorphology and structural evolution of the Corinth area of Greece. Philos. Trans. R. Soc. Lond. A 1985 (314), 379–407.
Wolf, L.W., Tuttle, M.P., Browning, S., Park, S., 2006. Geophysical surveys of earthquake-induced liquefaction deposits in the New Madrid seismic zone. Geophysics 71 (1), B223–B230.
Youd, T.L., 1984a. Geologic effects—Liquefaction and associated ground failure. Proceedings of the Geologic and Hydrologic Hazards Training Program. Open-File Report 84 760. U.S. Geological Survey, pp. 210–232.
Youd, T.L., 1984b. Recurrence of liquefaction at the same site. Proceedings of the Eighth World Conference on Earthquake Engineering, Earthquake Engineering Research Institute, San Francisco, Calif. 3, pp. 231–238
Youd, T.L., Perkins, D.M., 1978. Mapping liquefaction-induced ground failure potential. Proc. Am. Soc. Civ. Eng. J. Geotech. Eng. Div. 104 (GT4), 433–446.